(whether the fault is the Incirharman Fault or the Simal Fault) as to be mentioned later.

Assuming that it is the Simal Fault, the Simal Fault should be changing its direction suddenly from E-W to NNW around this point. If it is the Incirharman Fault, the Simal Fault should be displaced to the north on the west of the Incirharman Fault. In either case, the distribution of the Kozlu Formation is assumed to be expanding widely northward. However, the first interpretation looks rather odd regarding general features of the geological structure in this area. Therefore, the second interpretation looks more assuring; for its interpretation, drilling is required in the gallery No. 22929, which is nor underway by E.K.I.

(3) The conglomerate consisting of cobble to pebble size gravels encountered at 69.15 m of No. 2 hole is considered to be of the Karadon Formation in view of the size and contents gravels (the conglomerate of the Kozlu Formation is reportedly consisting of tranule to pebble sized gravels and does not contain the pebbles of red sandstone or igneous rocks) as well as in view of its surrounding rock facies and stratigraphy. The subsequent alternation of sandstone and conglomerate inserting the siltstone and a thin coal seam is characteristic of the rock facies of the Lower Karadon Formation. It does not contradict the fact that the fossil pollens in the coal seam indicate the Westphalian A, B (the Kozlu Formation and the Lower Karadon Formation). The dip of the Karadon Formation beyond the fault indicates 70 – 80° at the maximum, which means the said formation is sharply dipping. (The maximum dip of the core sample indicated 75°, while the angle of the drill hole to the horizon was 5°.)

2-5-B Geological interpreatation based on the drilling results

For interpretation of the drilling results of the two holes mentioned above, it would be necessary to elucidate the geology of deeper section of the Kozlu Mine. For this purpose, by compiling maps of mined out area of main coal seams, abandoned galleries and major geological sections, the structural contour maps have been drawn of the Sulu Seam, which appears in most galleries of the mine, for the currently working area and of the Büyük Seam, the uppermost operating coal seam of the Uppermost Kozlu Formation, for the area beyond the Simal Fault (Fig. 18)

Of the existing mine data, the geological sketches of most important galleries – the gallery No. 22727 at -300 m level, galleries No. 22925, No. 22926, and No. 22945 at -425 m level – have been reexamined and upon modification of the geological sections by each grid line made by E.K.I. with the data of the mined areas – the existing underground geologic maps

(the underground map of the Büyük Seam with the scale of 1/1,000, the maps of the Çay Seam and the Acilik Seam with the scale of 1/5,000), the geological sections of the Galleys No. 22925/22927, No. 22926 and No. 22929 in the directions of each gallery and the geological section of the grid line 47500E have been drawn.

Of the current mining area of the Kozlu Mine, the eastern half zone of the north wing of the Kozlu Dome, namely from the gallery No. 22923 eastward to the gallery No. 21945 (corresponding to the land area), bears the Simal Fault with a small throw and it is not so difficult to drill a gallery penetrating this fault. Thus, the Büyük Seam beyond the Simal Fault has been already mined through the levels between + 35 m and -350 m level (the exploratory adit have been driven to -425 m level).

However, toward the offshore area west of the gallery No. 22923, the throw of the Simal Fault becomes greater (presumably 600 – 700 m), the fault's fractured zone becomes wider (about 40 m wide in the gallery No. 22925 at -425 m level) and the earth pressure after excavation is higher. East of gallery No. 22923, blocks on both sides of the fault are hard sandstones with strong resistance to fracture. Therefore, there is only a little disturbance to keep the galleries not much deformed. Gallery No. 22925 has a wide fractured zone, presumably because of its shaly rock facies, having caused a remarkable swelling of wall.

The analysis of the above data on the geological block beyond the Simal Fault is as follows:

(a) The mining results of the Büyük Seam in the eastern area (east of the gallery No. 22923) indicate that, of the interval from +35 to -415 m, the coal seam dips at an angle of 40° between -200 m and -300 m and at an angle of 50° between -300 m and -400 m.

(b) Beyond the Simal Fault in Gallery No. 22727 at -300 m level, the Karadon conglomerate formation is sharply dipping at 60° – 80° (partly overturned).

(c) The Karadon conglomerate formation beyond the fault in Gallery No. 22926 – No. 2 hole also dips sharply at 60° – 80°.

From the above, it has been made clear that the geological block beyond the Simal Fault west of Gallery No. 22923 has a throw of 600 – 700 m as against the corresponding block behind the fault and that the block is dipping sharply at 60° – 70° near the fault.

Therefore the exploration work beyond the Simal Fault at the currently working level (-425 m level) is considered impossible in the western area (west of Gallery No. 22923) because no

coal seam is assumed at that level. The only possible way would be to explore the Büyük Seam, the uppermost coal seam having been mined in the eastern area, by means of horizontal drilling to be conducted before the Simal Fault when the mining of this area goes down below -550 m level.

On the other hand, on the west block of the Incirharman Fault, the Simal Fault is assumed, as mentioned earlier (IV-2-5. A. (3)), to have been displaced to the north by the Icirharman Fault. Drilling from the heading of Gallery No. 22929 is required to obtain information on how much the Simal Fault is displaced. E.K.I. is now managing a horizontal drilling (hole No. 3) with the drilling machine EP-1W from heading of the gallery No. 22929, being extended by about 80 m, to confirm the exact location of the Simal Fault and, if penetration of the fault is successful, the structure of the geological block beyond the fault will be clarified.

2-6 Coal Reserves of the Kozlu Mine Beyond the Simal Fault

As mentioned in IV-2-5, in the geological block beyond the Simal Fault, the Büyük Seam east of Gallery No. 22923 has already been mined from near the top of the fault to around -350 m level. Its deeper portion is kept from mining in consideration of a possible mining pollution to the civil constructions. The eastern mined-out area corresponds to the land area, but the western area corresponds to the offshore area. By considering the safety for sea water encroachment, the shallow portion of this area has been left as a safety pillar.

The geological structure of the Kozlu Mine beyond the Simal Fault is shown in Fig. 18, the structural contour map of the Buyü Seam. Whether there are other minable coal seams besides the Büyük Seam in this area is not known from the existing geological data. In view of the current working area where there are three major working coal seams of the Çay (Two or three step slicing method), the Acilik (Two step slicing method) and the Sulu in ascending order and where other minor coal seams are being mined only where the seams are developed, and where the interval between the Sulu Seam and the Büyük Seam is about 380 m (Refer to Fig. 29), it would be impossible to estimate the existence of minable coal seams without direct prospection. Therefore, the estimate of the coal reserves in the area beyond the Simal Fault has been done only on the Büyük Seam based on the following assumptions (Refer to Fig. 25):

(a) The area to be calculated of the coal reserves shall cover an area of about 3.8 km from

the Karadon Fault on the west to about 4 km east of Gallery No. 22945 where the Simal Fault intersects roughly in the WSW-ENE direction, and shall be divided into three blocks, A, B, and C from the east. (The distribution status of the Büyük Seam has been estimated on the basis of only a few geological data and is subject to change greatly depending on the future prospecting.)

(b) Block A is the deeper part of land area. In view of the possible subsidence by mining and the current drilling status of the galleries, calculation was made on the interval from -475 m to -1,000 m level.

Block B is the offshore deeper area up to the Incirharman Fault. The shallow part west of Gallery No. 22923 above -475 m level was excluded from calculation, taking into consideration, as mentioned above, of possible mining pollution and possible sea water invasion in the shallow mining. Then the interval from -475 m to -1,000 m level was taken into account for calculation.

In Block C, the location of the Simal Fault is not confirmed but has been tentatively assumed as shown in the figure, which indicates that the Büyuk Seam occurs only in deeper section than -700 m level. Accordingly, calcuation was made on the interval between -700 m and -1,000 m level.

(c) Since there was no information on the coal thickness of the deeper Büyük Seam, the average seam thickness of 2.5m in the upper working area was used in calculation (the coal thickness being 2.2 m). And the specific gravity of raw coal was estimated at 1.4.(1)

(d) Since the Büyük Seam in the concerned area is estimated to be sharply dipping with an angle of over 50°, the particular mining method should be taken into consideration and therefore its recoverable ratio cannot be fixed, and also, as mentioned above, the yield of the coal seam itself is not known. Consequently, only the coal reserve in place was calculated.

The estimated coal reserve in place of the Büyuk Seam is about 6.28 million tons as shown in Table 30. Theoretically, the calculation of the coal reserves in Block A, the deeper zone from the mined out area, should be discriminated into the proven, the probable, and the possible reserves in accordance with the distance from its confirmed line. However, as it was considered controversial whether the JIS (Japanese Industrial Standards) plan should be applied to a mine in Turkey, this report treated only the coal reserve in place.

---

(1) The clean coal yield in the Kozlu Mine is only 53 % (1980), and although the specific gravity of raw coal is considered above 1.4, the figure 1.4 was adopted for safety calculation.

Table 30 Reserve Calculation Table of Büyük Seam at the Kozlu Mine

Block	Area ($1000m^2$)	Inclinat.	Seam Thickness (m)	Specific Gravity	Coal Reserve In Place (1000 m.t.)	Remarks
Block A	821	48°	2.50	1.40	4,293	-415 ~ -1000m
Block B	376	63°	2.50	1.40	2,898	-475 ~ -1000m(East) -650 ~ -1000m(West)
Block C	214	50°	2.50	1.40	1,165	-700 ~ 1000m
Total	810				8,356	

3. OFFSHORE GEOPHYSICAL SURVEY

3-1 Data Acquisition

The offshore geophysical survey was carried out by SISMIK-1, M.T.A.'s survey vessel during the period from August 23rd to September 12th, 1981 on the basis of the seismic line program (Fig. 30) and the specifications planned by the preliminary survey team in March 1981.

Seismic coverage consist of 8 JICA lines (233.45 km) and 13 supplemental lines (246.175 km) totalling 21 seismic lines and 479.625 km in seismic coverage.

Gravity and magnetic survey as well as the seismic reflection survey were simultaneously carried out.

3-1-A Abstract scheme of the field operation

Commencement of the survey was delayed due to inconvenience of the M.T.A., compressor trouble, and bad weather, etc. Shooting for JICA's originally proposed lines was started on August 1st or 23rd, 1981 and completed on September 12th, 1981. Survey duration for the supplemental lines was from September 15th to September 20th, 1981.

Tables 31 and 32 show seismic line number, its coverage and specification of the field operation. The original specification of the field operation (Item-1, 2 and 3 in Annex-2, Refer to Minutes of Meeting, March 27, 1981) was somewhat changed by M.T.A.'s own decision and this was thought to be a reasonable modification when the efficiency of the field work and restricted performance of TIMAP computer system were taken into account.

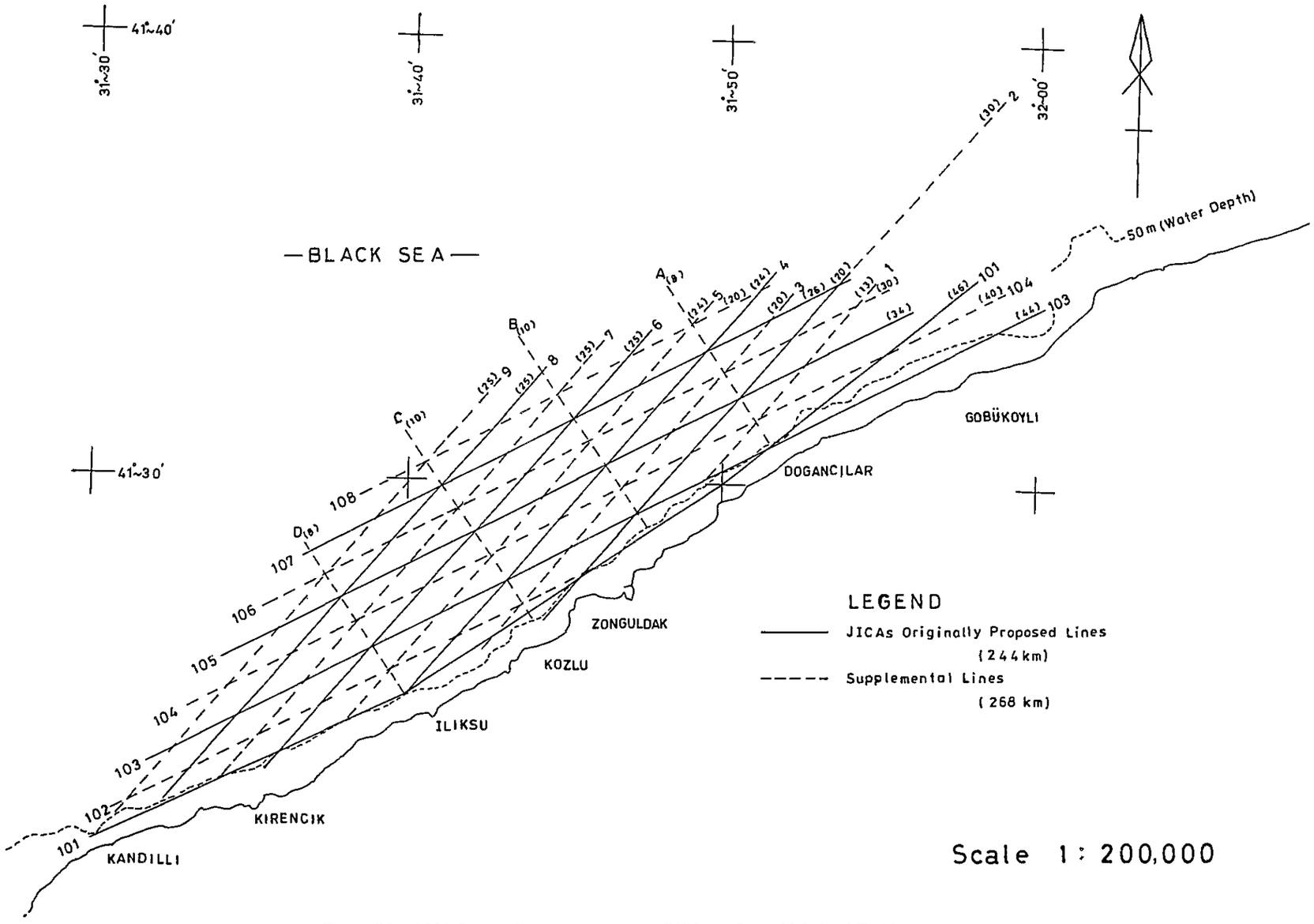

Figure 30 1981 Survey Program Map in the Offshore Zonguldak Cool Field

Table 31 A Table of Survey Line Length

JICA'S ORIGINALLY PROPOSED LINES			
Line No.	Programed Length (km)	Final Length (km)	Direction
Line 2	20	20.800	NE – SW
" 4	24	23.725	NE – SW
" 6	25	24.075	NE – SW
" 8	25	24.925	NE – SW
" 101	46	34.375	NE – SW
" 103	44	44.925	WSW – ENE
" 105	34	33.625	WSW – ENE
" 107	26	27.000	ENE – WSW
Total Length	244 (km)	233.450 (km)	

SUPPLEMENTAL LINES

Line No.	Programed Length (km)	Final Length (km)	Direction
Line 1	13	12.175	SW – NE
" 3	20	20.200	NE – SW
" 5	24	24.225	NE – SW
" 7	25	23.225	NE – SW
" 9	25	22.050	
" 102	25	23.675	WSW – ENE
" 104	40	40.100	ENE – WSW
" 106	30	30.100	ENE – WSW
" 108	20	16.800	
" A	8	7.600	NW – SE
" B	10	9.125	NW – SE
" C	10	9.000	NW – SE
" D	8	7.900	NW – SE
Total Length	258 (km)	246.175 (km)	

Table 32 Specification of the Offshore Geophysical Survey

Survey vessel	MTA SISMIC-I(720 GWT)		
Seismic Instrument	TI DFS IV		
	Filter	8 HZ – 124	HZ
	Constant Gain	24	db
	Sampling Rate	2	msec
	Record Length	3	sec
	Channel Number	48	
	Format		SEG-B(1600 bpi)
Seismic Source	Bolt AIR GUNS (40, 20, 10 cubic inches)		
	Total Size		70 cubic inches
	Pressure	1800 – 2000	psi
	Depth	5	m
	Shot Interval	25	m
Compressor	APS-D20B-500 x 2		
Geophone	SEC Streamer Cable		
	Group Interval	25	m
	Cable Length	1200	m
	Number of Hydrophone Group	20	
	Depth	5 – 6	m
	Number of Sea Bird	4	
	Near Offset Distance	32	m(JICA lines)
		10	m(Supplemental lines)
	CDP	24	fold
Positioning Instrument	TRISPONDER DEL NORTE TECHNOLOGY, INC. Model 217C(210 Series)		
Gravity Meter	Lacoste and Romberg Air/Sea Gravitimeter Model-S		
Magnetometer	Barriger M-123 Recording-Magnetometer		

3-1-B Test shot

Test shot was carried out prior to the filed survey and part of its was conducted after the survey. Most of the test shots (Item 2 and 3 in ANNEX-3) were carried out on August 8th & 9th, 1981. Observation of air gun outgoing signature (Item-1 in ANNEX-3) and high resolution test (Item-4 in ANNEX-3) were carried out on September 20th. All the tests except observation of air gun outgoing signature were shot on Line-2.

3-2 Data Processing of Seismic Reflection Data

Due to the delay in delivery of the field type to M.T.A., data processing was commenced on September 7th, 1981, a little behind the schedule. This processing work was completed by the united efforts of all members of Seismic Data Processing Section in M.T.A. The computer system used for this processing was TIMA 980-B designed and constructed by GSI, USA. Fig. 31 shows it's Block diagram. A soft ware package used was MATE-5000, SCA, USA, slightly modified by BP, UK. in order to improve its function. Author's work started with the preparation of time schedule. First, performances available with TIMAP

980-B examined and at the same time, various parameter for deconvolution were determined using Line-2 as a test line. Table 33 shows the performances of TIMAP computer system.

Table 33 Processing Faculty of TIMAP System at M.T.A.

1) Demultiplex(including Gain Recovery)	3.5 hours/20 km
2) CDP Sorting	2.5 houts/20 km
3) Velocity Analysis (1.25 km Interval) (Constant Velocity Stack, 10 traces, 29 Velocities) Including DCON + Band Pass Filter	2.7 hours/20 km
4) Low Cut Filter + DCON + AGC +NMO CORR. + Mute + Stack	6.3 hours/20 km
5) DCON + Band Pass Filter	0.5 hours/20 km
Total	15.5 hours/20 km

Remarks: Sample Rate : 2 msec
Shot Point Interval : 25 m
48 channel/24 fold
Processed Record Length : 3 sec for 1) – 3), 2.5 sec for 4), 5).

The completion of all the processing work during the Author's stay at M.T.A. was thought to be somewhat difficult due to lack of time with the occurrences of electric power failure and restricted performance of TIMAP system. As a result of consultation with Mr. Necati GURCAN, they finally decided to extend their working time. As a matter of fact, operation of processing was carried out by shifts from September 16th.

3-2-A Method of data processing

Figs. 31 and 32 indicate the flow of the data processing used for the present study.

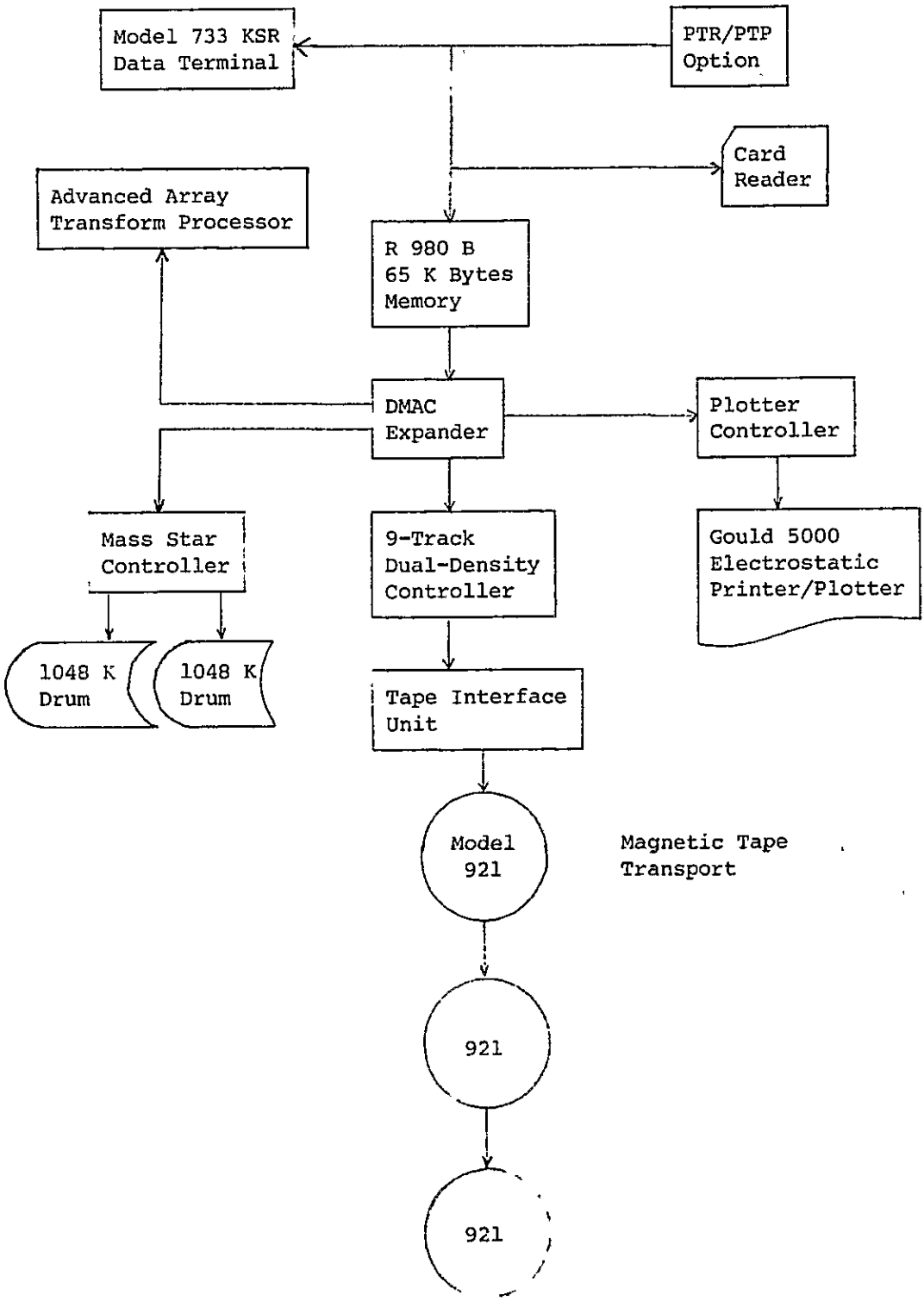

Fig. 31 The Organization of TIMAP System Hardware at M.T.A.

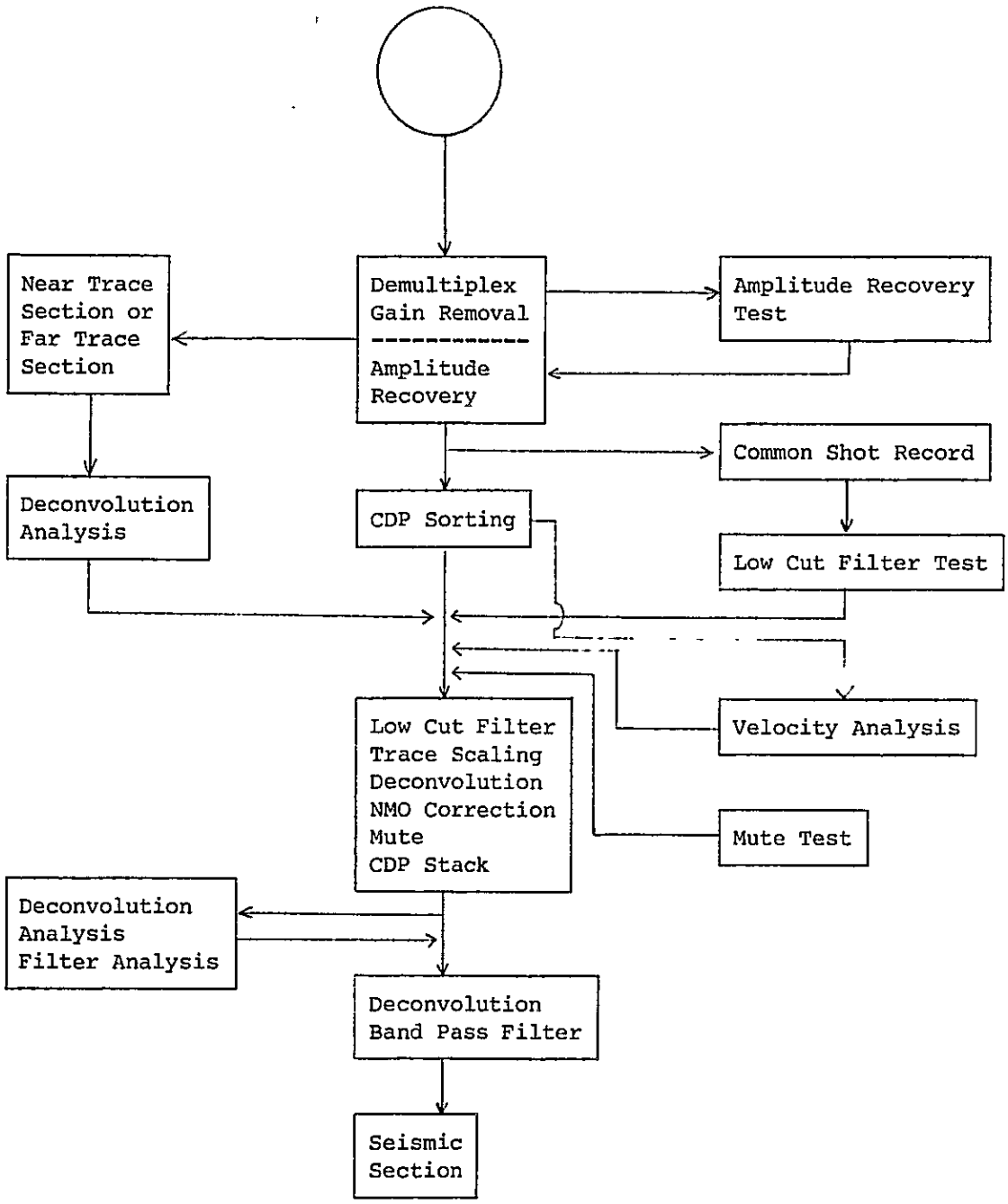

Fig. 32 Flow Diagram of Basic Processing at MTA

Processed record length before the stack records was 3 seconds and after stack record, was 2.5 seconds. In the beginning, the sampling data of 2 milli-seconds was used for some of the lines, but later the data were sampled at the rate of 4 milli seconds since the result of the Band-pass filter test indicated that 4 milli second sampling rate was sufficient enough for reconstructing the conventional stacking record. After finding this, sampling rate of 2 milli seconds in the stage of demultiplexing was also changed to 4 milli second sampling rate in order to save time. Table 34 shows the length of the seismic lines and the sampling rate used for every seismic line.

Table 34 The Items of Reprocessing Lines

JICA'S ORIGINALLY PROPOSED LINES		
LINE NO.	SEISMIC COVERAGE	SAMPLING RATE
Line 2	20.800	2 msec
Line 4	23.725	2 "
Line 6	24.075	2 "
Line 8	24.925	4 "
Line 101	34.375	4 "
Line 103	44.925	4 "
Line 105	33.625	2 "
Line 107	27.000	2 "
Total Coverage	233.450 (km)	

Major part of the data processing used for the present study are summarized as follows:

(1) Demultiplexing and gain removal (Except for the data recorded with constant gain)

(2) True amplitude recovery

The method o amplitude recovery used was based on the formula

$$A \alpha e^{-\alpha t}$$

(Time 0 sec : 0 db, Time 3 sec : 20 db)

(3) Common depth point sorting

CDP traces were sorted together according to the shooting and recording logs.

(4) Low cut filter

Since the streamer cable was towed at relatively shallow depth aiming to increase the resolution, a significant low frequency noise was observed on the seismic record. Dominant frequency on the seismic record was tested and finally, a low cut filter which cuts the frequencies lower than 12 Hz was used.

(5) Trace scaling

Use of the low-cut filter resulted in rapid attenuation of amplitude of seismic wave with respect to time. Aiming to emphasize the small signals and to increase the effect of deconvolution, a kind of automatic gain control system (scaling : Digital AGC) was used.

(6) Deconvolution

After making a deconvolution test, the parameters of deconvolution before stacking were determined as follows:

i) Operator length : 300 m/sec

ii) Spiking deconvolution

iii) Gate length of auto correlation : 2,000 m/sec

(7) Velocity analysis

Since most of the investigated area was covered by high velocity layers, refraction multiples and water reverberations were dominant on the seismic record while important primary reflections were very weak. Therefore, after checking the performance of M.T.A.'s software package for velocity analysis, the constant velocity stack method was employed and velocity analysis was carried out at the interval of every 1.25 kilometers taking M.T.A.'s software package for velocity analysis into accounts.

Careful attention was paid to the velocity analysis. The final stacking velocities were determined, taking velocities and depth which were derived from the refracted arrivals into consideration.

(8) NMO Correction, Mute and CDP stacking

The stacking velocities determined by velocity analysis were interpolated linearly in the direction of time and distance and after determination of the final velocities of every location, NMO corrections were conducted.

Muting was carried out in an attempt to eliminate the refraction multiples.

The parameter of the muting was determined as shown in the following figure.

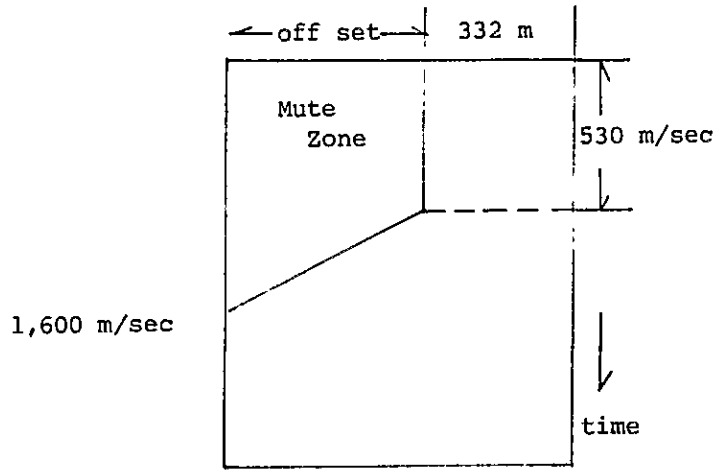

Parameters used for Muting

(9) Deconvolution after stack and band-pass filter

After a deconvolution test was carried out with raw stacked section, it was decided to apply deconvolution again for the stacked data.

Parameters of deconvolution after stack were as follows:

i) Operator length : 300 m/sec

ii) Predictive Deconvolution

iii) Predict distance : 16 m/sec

iv) Gate length of the auto correlation : 200 m/sec

A band pass filter test was also carried out and it was finally decided to use a non-time-variant band pass filter ranging from 15 HZ to 70 HZ.

3-2-B Examination of the processing result

According to the velocity information from the refracted arrivals, within the shallow area down to 80 meters in depth or several kilometers off the coast, velocities of the formation of the seafloor or of immediately below the seafloor range from 3,500 m/sec to 4,100 m/sec. Judging from the data of onshore geology, most of these formations are considered to be limestone of the Cretaceous age. Reflected events from the formations underlying the limestone were very weak in its amplitude. For this, several causes could be considered:

(1) The primary reflections tend to be masked by the very strong multiple reflections (including refraction multiples and multiple refractions) which resulted from the high velocity layer immediately below the seafloor.

(2) Most of the acoustic energy are reflected back to the surface of the seafloor because

the reflection coefficient at the seafloor is quite high. For example, it reaches 0.5, if 1,450 m/sec and 4,000 m/sec are assumed as the velocities of the seawater and the seafloor formation respectively. Accordingly only small amount of the acoustic energy can be penetrated into the sediments.

(3) Since the incident angle of the wave front is very small, the ratio of the total acoustic energy emitted from the sound to the energy which can be propagated into the sediment is only 20 percent in comparison with the usual sedimental condition.

(4) Complicated geological structure

In order to increase the incident angle, use of a long air gun arrey can be recommended theoretically. Occurrence of the low velocity layers (about 1,600 ~ 1,800 m/sec in interval velocity) were recognized clearly on some seismic line (e.g. line 4) in the shallow region between the continental shelf and slope. The sea bottom topography in deep sea area, ranging from 200 to 1,100 meters in water depth is extremely complex and also the geological structure is complicated in the deeper sequences and therefore the reflection events could not be well traced in those regions although some partial indications of reflections could be recognized.

All seismic data have been processed taking particular geological settings of the area into consideration and paying special attention to the velocity analysis. As a result of this, conventional processing for about 200 kimometers of seismic coverage including attacking records could have been completed. Concerning the special processing, only time-migration processing could have been achieved due to insufficient performance of hardware and software. Fig. 33 shows an example of the conventional processed sections.

3-3 Purpose of Interpreting the Seismic Reflection Data

3-3-A Purpose of interpreting the seismic reflection data

The main purpose of interpreting the reflection data was to clarify the subsurface structure of the Carboniferous including the main coal seam in the area off the coast of Zonguldak coal field. Also, technical training for M.T.A.'s geophysicists was also aimed, while conducting the interpretation.

3-3-B Procedure used for the present interpretation

(1) Plotting the intersections of the seismic lines on the seismic time sections.

In spite of the fact that every reflection time at the points of intersections of seismic lines should coincide between the corresponding seismic lines, a relatively big difference in reflection time from seafloor were found at the beginning of the interpretation. It was found after spending more than ten days that this discrepancy was due to mis-plotting of the shot point number on the seismic sections. The checking the reflection time at every intersections was an unavoidable procedure even though relatively long time have been spent to solve this problem because final accuracy of the interpretation was largely dependent on this correction.

(2) Detection of the reflection events

Considerable efforts have been devoted to detect the seismic events on the final sections processed at M.T.A.'s seismic data processing section. However, selecting events was somewhat difficult due to insufficient occurrence of the events and its poor quality.

Concerning the quality of the processed data, the final sections processed by JAPEX in 1981 appeared to be better than those processed by M.T.A. This was presumably due to the fact that the performance of M.T.A.'s software package (MATE-500) was limited in controlling the processing parameters in comparison with JAPEX's software package and due to insufficient contrast of seismic sections displayed by the DOT-PLOT type electro-sensitive display unit. Only two reflected hoirzons were recognized, one ranging from 0.2 to 0.3 seconds (Horizon-green) and the other from 0.4 to 0.6 seconds (Horizon-brown) in two-way time. Reflection events from farther deeper horizons could not be detected.

(3) Identification of the reflection time at intersections

In general, reflection time at the intersections agreed well with the reading on the other lines after the location of shot-point number on the sections were corrected. When the

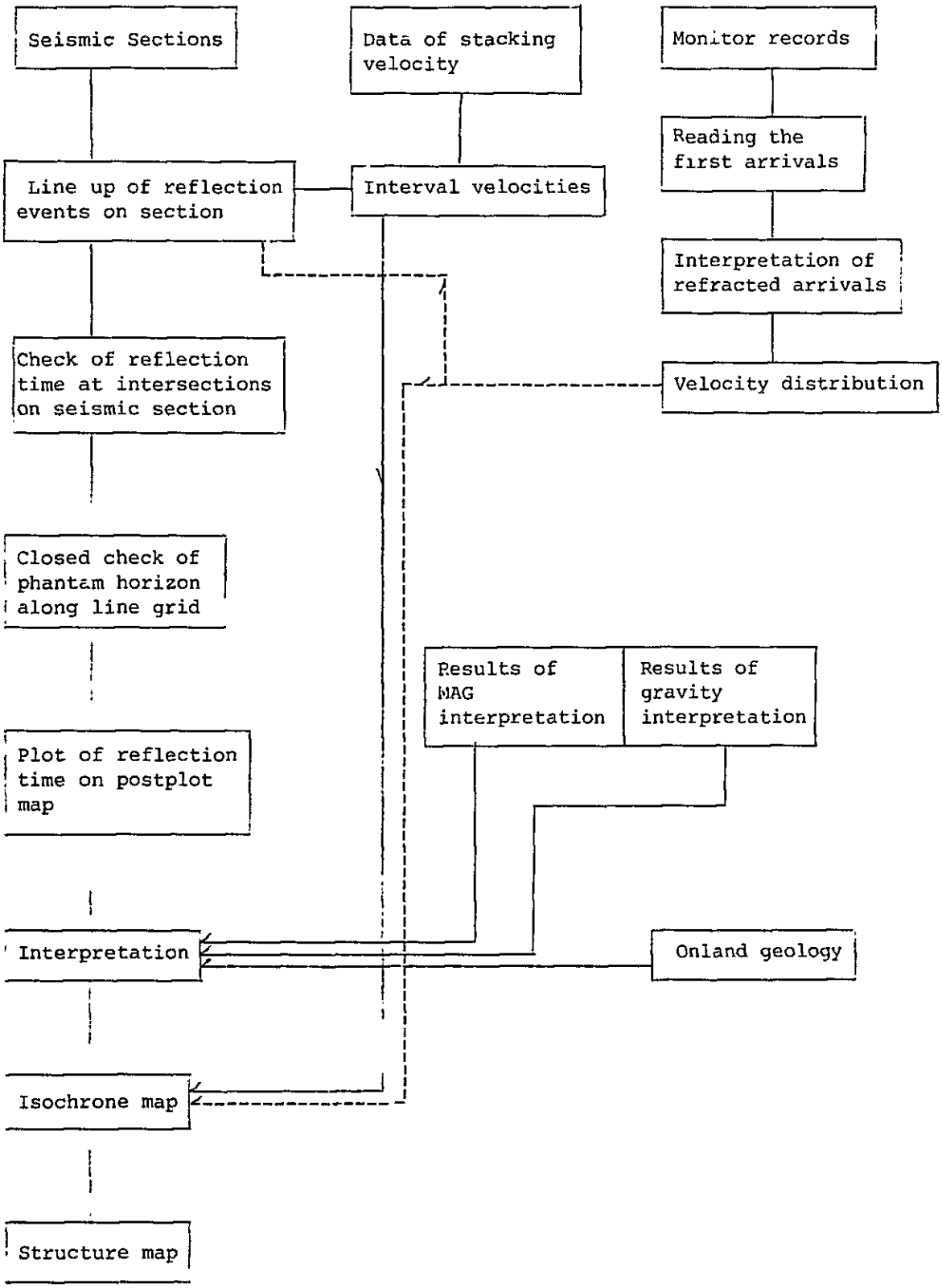

Fig. 34 Flow of Seismic Interpretation

reflection events on one of the interesecting sections were so weak that precise reflection time was unreadable while those on the other line were relatively clear, correlation of reflections was based on the events of better quality.

(4) Check of picked events by loop tying

A reflection characterized on the seismic section by a single trough or single peak often evolved into two or three trough over several traces. Such change in wave form was considered to be caused by the effect of superimposing noise on signal. However, a lateral geological change could also be considered as well as other possible cause of such phenomenon. Consequently to decide which one of following trough should correlate with the one from which their branch was very important. This type of discontinuity in correlating the reflection events were found at many places throughout the survey area and made the interpretation difficult. To solve this difficulty, reflection events were correlated along a loop which was constituted by a combination of four seismiclines starting from an intersection, along one line to another and around to its starting point. (Fig. 35) In Fig. 35, a, b, c and d are intersections of seismic lines, reflections at intersection a were identified and checked comparing section of line-4 and line-107. Correlation of reflections then was followed along the section of line-107 to the intersection b. At b, the selected events were checked and compared to those represented on the section of line-3 and events were again followed along the section of line-3 and so on. If selected events were not on the same level when correlation got back to its starting point a, selection must have been wrong somewhere. To correct this sort of mis-tie, reflections were recorrelated at a point where a difficult decision has been made and tried in another way. This trial is repeated again and again until the selected events were on the same level when correlation got back to its starting point a. To achieve this procedure, relatively long time was consumed. This sort of correlation was not always as simple as it may appear, because the shape of reflection was not purely isolated single pulse but always associated with wave train. Also a number of fault-like pattern on the sections made difficult the selecting of the phase of reflection events.

(5) Plotting the reflection time on the post-plot map.

A number of reflection time measured from the record section were plotted at every shot point location on the post-plot map.

(6) Drawing of the isochrone map

Plotted time were contoured and an isochrone map (1:50,000) was prepared.

(7) Time-depth conversion and the preparation of the structure map

Conversion from reflection time to depth was carried out, assumming the average velocities to horizon green and brown were 2 km/second and 4 km/second, respectively.

Determination of velocities was, of course, one of the most important procedure in seismic interpretation because accuracy of the final result of depth sections was dependent on the reliability of the velocities used for the time-depth conversion.

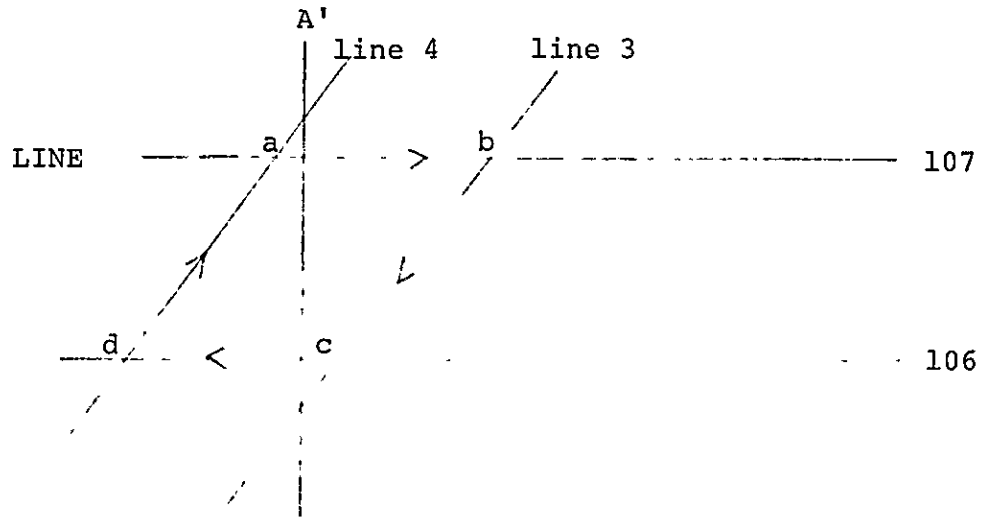

Fig. 35 Procedure of Reflection Line-up

In general, a sonic log data acquired in an exploration well which is located on one of the seismic lines provide absolutely perfect knowledge of the velocities and when sonic log data are not available, stacking velocities from the CDP ensemble is used as another approach to obtain the velocity value. However, sonic data was not available and velocity information from the reflection data was thought to be insufficient for the present study since the occurrence of primary reflections was limited compared to other low velocity events and refraction multiples. In 1981 when the seismic data were reprocessed in Japan, the same difficulty was faced in determining the velocities from the reflection data, and the velocities were determined experimentally, judging from the final effectiveness of stacking assuming several velocity models. Finally, the velocity of 4 km/second (K-velocity) could have been obtained. For the present interpretation, this value was chosen again as a r.m.s. velocity to the top of Horizon-brown. But for the shallow portion, to the top of Horizon-green, velocity of 2 km/second was chosen from the viewpoint of the result of refraction survey and onshore geology.

3-3-C Result of the Interpretation

Seismic situation map (Fig. 1). isochrone map (Fig. 36) and the structure map (Fig. 37) are attached to this report. The result of the interpretation of reflection seismic data are outlined as follows:

(1) Reflection observed events and its geological correlations

Two reflection events were recognized. One of them, called Horizon-green, was found ranging from 0.2 seconds to 0.3 seconds in a two way reflection time throughout the investigated area and the other, called Horizon-brown, from 0.4 seconds to 0.6 seconds. Horizon-brown was generally inferior in quality to Horizon-green and was characterized by restricted occurrence in the area 3 to 4 kilometers off the coast. Judging from the conformable relationship observed between these two horizons as well as the onshore geology, it was considered that Horizon-green could be correlated with some upper part of biotite andesite in the upper Cretaceous (Campanian stage), and Horizon-brown with the part around the base of Agglomerate (Santonian – Coniacian stage).

Reflection events from the deeper horizon could not be recognized throughout the area.

(2) Thickness between the Horizon-green and Horizon-brown.

When 2 km/second and 4 km/second were assumed as r.m.s. velocities to the top of Horizon-green and Horizon-brown respectively, the thickness interval between these horizons was calculated to be in the range from 700 meters to 1,000 meters and the resultant dip, appeared to coincide, with good approximation, to those inferred from the onshore geology.

(3) Estimated structure of the Palaeozoic

Structure of the Palaeozoic could not be delineated, as described before, due to the absence of reflected arrivals. According to the onshore geology, however, the structural high of the Cretaceous tend to be underlain by the relative high of the Palaeozoic. If this tendency can be applicable to the offshore area, the Palaeozoic can possibly occur at relatively shallow portion in the area of the Cretaceous high, but the present knowledge was insufficient to permit any definite conclusions.

(4) Horizon-green

In macroscopic view, Horizon-green has a SW-NE trend parallel to the coast line. In the area off the coast from Zonguldak to Kilimli, a northerly trending nose-like structural high was recognized. At the most northern part of the investigated area,

there was an indication in which the above-mentioned general trend tend to bend toward the westeast direction.

On the other hand, similar trend could be observed southwest of the estuary of Filyös river. This may suggest that the Cretaceous of the Zonguldak coal field forms a huge anticlinal structure which runs approximately parallel to the coast line as anticipated.

The northern flank of this anticline appears to be situated in the offshore area.

Horizon-green dips gently toward the north in the area near the coast line and suddenly dips steeply approximately 4 kilometers off the coast line. If the structural relationship between the Cretaceous and the Palaeozoic which have been recognized in onshore geology holds, then the coal bearing formation is considered to deepen steeply to the north from this area. A couple of half-basin-like deep zones were found to the northwest and northeast of Zonguldak, where the above mentioned local high was located dipping gently toward the north.

(5) Horizon-brown

Reflection events from the Horizon-brown could be recognized only within the area three to four kilometers from the coast. In this extent, Horizon-brown conformably underlies the Horizon-green and has a general trend that is parallel to the coast line.

In the area off Kozlu-Zonguldak a nose-like structural high was also recognized. Its 1,000 meters level extends north-north westward over a distance of nearly 4 kilometers off Zonguldak. Off the coast from Iliksu to Kirencik which is southwest of Zonguldak, and off Kilimli which is northeast of Zonguldak, the structure high extends over a distance of 2 kilometers and 3 kilometers, respectively. Horizon-brown dips gently down to about 1,200 meters in depth. It was difficult momentarily, to distinguish whether the Horizon-brown dips northward continuously with the same angle or dips steeply farther north from this level since any reflection events could not be traced in the area beyond this level.

(6) On the nose-like structural high

The contour lines of the nose-like high recognized on both Horizon-green and brown show apparent conformable relationship between them in the area northwest off Zonguldak, but in the area off Kilimli, the contour lines of Horizon-brown has a different pattern to that of Horizon-green and an indistinct fault pattern was found at the southwestern flank of the high. There may be a possibility that this fault extends

southward and, after changing its direction, connects to a east – west trending gentle strike fault which was observed onshore in the visinity of Catalağzi.

(7) Relation to the gravity survey

There was no correlative relationship between both Horizons-green and brown and the result of gravity survey. This may be due to the fact that the gravity anomalies expressed deeper information than the two horizons representing the upper and middle Cretaceous.

(8) Relation to the magnetic survey

The magnetic anomalies developed from the analysis of the magnetic data was considered to be caused mainly by the distribution of Agglomerate (Santonian – Coniasian stage) in the middle Cretaceous which was close to the seismic Horizon-brown. (nearly the base of the agglomerate)

A contour line which represents the center of the maximum magnetic high runs nearly parallel to the coast and appears to have somewhat similar general trend pattern to the 800 meter level of the seismic Horizon-brown. (M.H. on Fig. 58)

3-3-D Summary of the interpretation of the reflection seismic data

(1) Green and Brown horizons were considered to correspond nearly to the top of BIOTITE ANDESITE in the upper Cretaceous and nearly to the base of agglomerate in the middle Cretaceous, respectively.

(2) Any reflection events from the Palaeozoic could not be recognized. However, judging from the onshore geology, it was considered that the area of structural high at the green horizon may be underlain by the relative high of the Palaeozoic.

(3) The Cretaceous, in general, has a trend that is parallel to the coast line.

At the northernmost part of the area, the general trend pattern appears to be bending toward W-E direction. Taking the data of onshore geology into account, it was considered that the Cretaceous forms a high anticline and its northern flank is situated off the coast line.

Horizon-green dips gently northward over a distance of nearly 4 kilometers from the coast and from there dips steeply northward. Horizon-brown also dips gently toward the north to the area nearly 4 kilometers off the coast line. The structure of Horizon-brown beyond 4 kilometers off the coast could not be traced.

(4) A nose-like structural high was recognized in the area off Zonguldak. If the structural relationship between the Cretaceous and the Palaeozoic on land (which have been

acquired from onshore geological survey) is applicable to the offshore area, coal bearing formation is considered to occur at a relatively shallow portion in the area of the Cretaceous high.

(5) It was considered that the general pattern of the noselike structural high which was accompanied with a couple of the half-basin-like deep zones on both flanks resulted from the folding or folding associated with faulting. Even in the lattercase, however, the fault might have a relatively low angle judging from the fact that clear fault patterns were not recorded on the seismic sections in this region.

(6) There was no correlatable events between the seismic and gravity results because the gravity result presumably reflected deeper information than the seismic information.

(7) Horizon-brown appears to correspond to the magnetic anomalies which runs nearly parallel to the coast line. A contour line which represents the center of the maximum magnetic high has a somewhat similar pattern to the 800 meters level at the Horizon-brown.

3-4 Analysis of Velocity Distribution of Sea Floor

3-4-A Purpose

The analysis of velocity distribution by the refraction method using the monitor records acquired in the reflection seismic survey is to obtain knowledge on the relationship between the distribution of seismic velocity and the corresponding lithological nature.

3-4-B Method of analysis

The assumptions of the velocity analysis, especially for the propagation of seismic waves in layers, are summarized as follows;

a) The seismic wave velocity in the homogenious medium (velocity layers) is constant for every direction.

b) The propagation of the seismic wave in the layer is to be followed by Fermat's principle, i.e. the propagation path of the seismic wave between two arbitrary points will take a minimum travel time. In other words, the above mentioned assumptions are described by the following fundamentals:

i) The propagation path of the seismic wave in the same velocity layer is to be straight.

ii) The seismic wave reflection at the boundary between the different velocity layers and the angle of incidence is equal to that of reflection.

iii) The seismic wave refracts at the boundary between the different velocity layers according to the Law of Refractions which is identical to the term in optics known as Snell's Law.

To recapitulate the Law of Refractions,

$$\frac{\text{Sin}\,\theta_1}{\text{Sin}\,\theta_2} = \frac{V_1}{V_2}$$

θ_1 : Angle of Incidence
θ_2 : Angle of Refraction

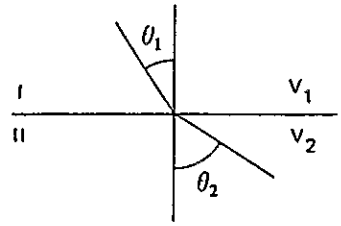

iv) Under the above condition, the propagation path of the seismic wave is reversible and the travel time(T) on the path is the same for both ways.

$T_{ASRB} = T_{BRSA}$

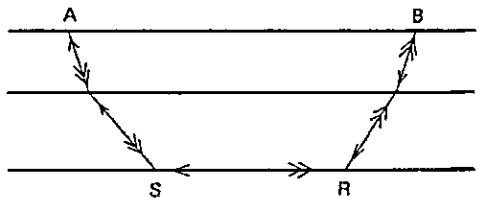

Fig. 38 shows examples of records used for analysis.

Usually, in the analysis of the refraction method, as the travel time of P-wave will be read off from the monitor record as a propagation time which is the first arrival time of P-wave, a Time-Distance (T-D) curve will be made for the refraction analysis.

The T-D curve is composed of the horizontal distance between the shot point and the receiving point put on the horizontal axis, and the first arrival time on the vertical axis. (Fig. 40) But in this case, the T D curve obtained from the monitor record is only a one way curve. Therefore, to carry out the refraction analysis, it is necessary to have the T-D curve of the opposite direction started at the corresponding shot point at the opposite side. But utilizing the above mentioned principle iv), a pair of T-D curves can be obtained.

The following is the refraction method used in the analysis of the model of the two strata velocity layers.

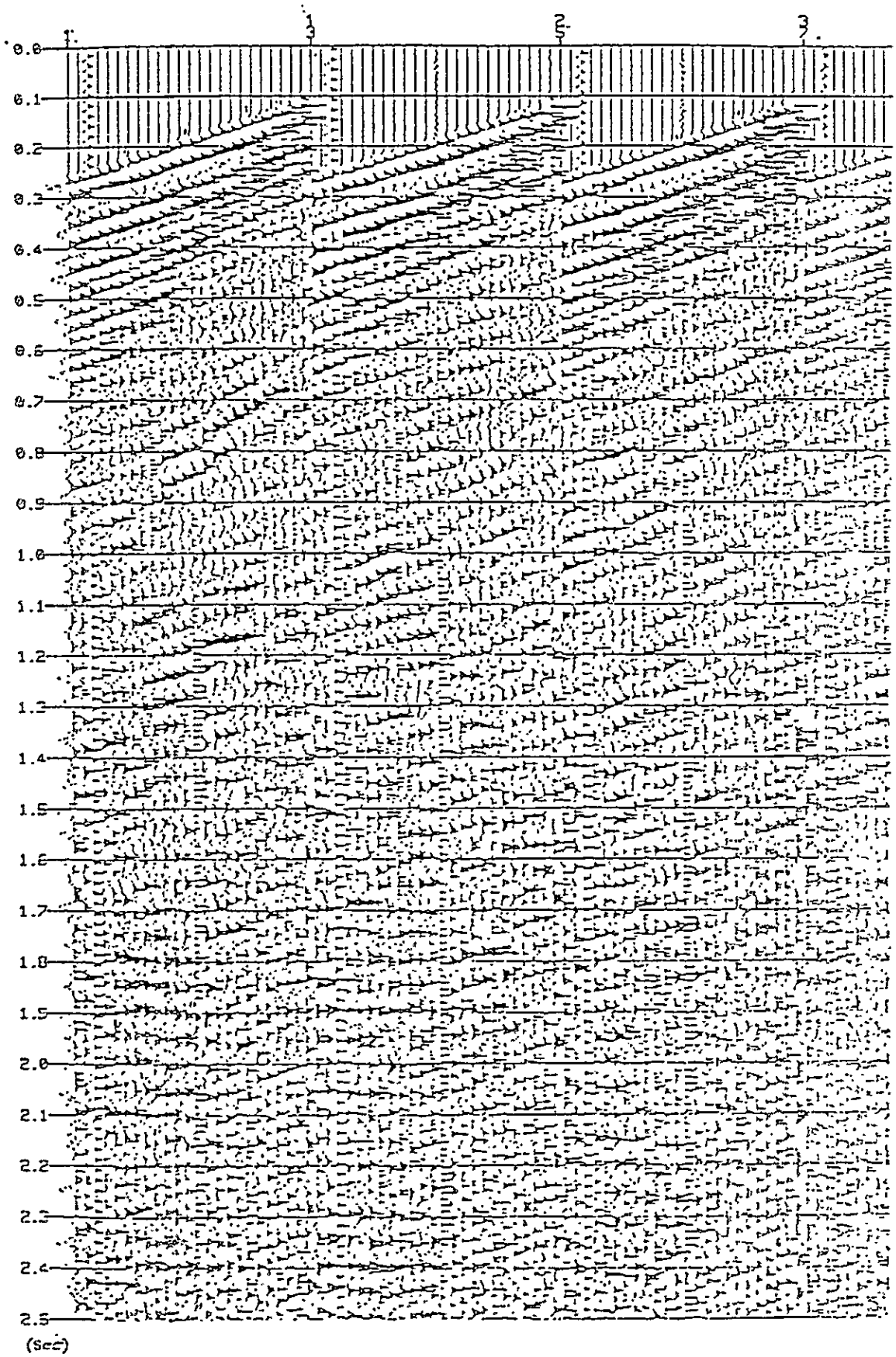

Fig. 38 Examples of seismic records

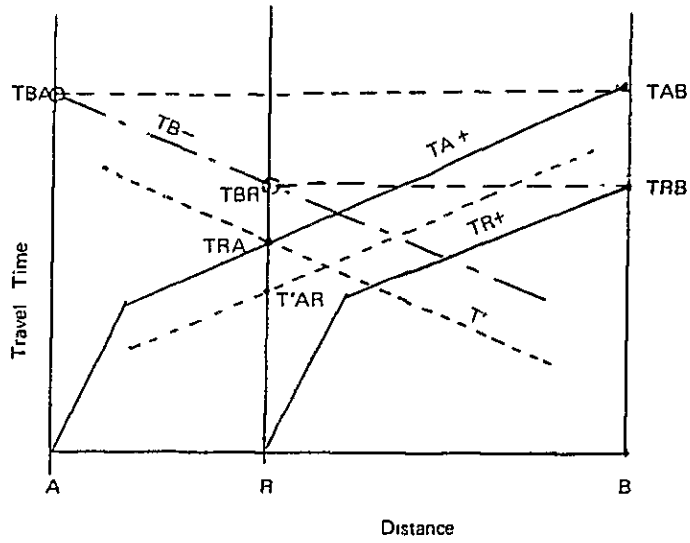

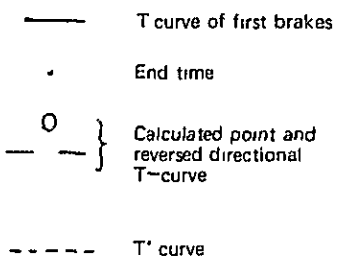

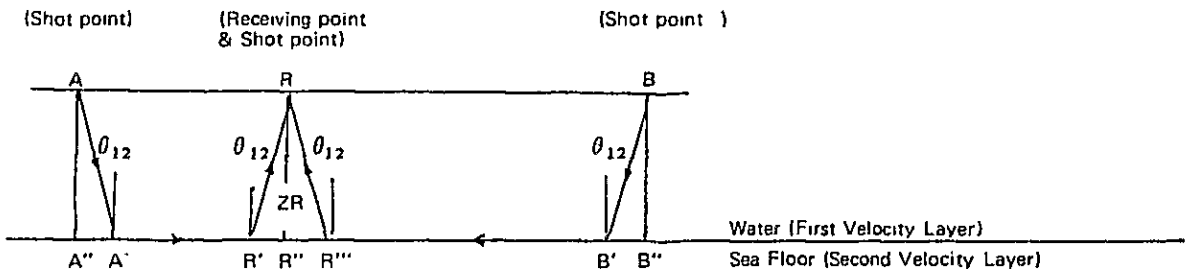

Fig. 39 Explanation of the T-D Curve & Velocity Section

Now

Z_R : the thickness of the upper medium at the receiving point R

T_{AR} : the sum of the travel time passing between the path of A–A′–R′–R

then

$$T_{AR} = D_{1,2}(A) + D_{1.2}(R) + \frac{A''R''}{V_2} \tag{1}$$

under

$$D_{1,2}(A) = D_{1,2}(R) = \frac{Z_R \cos\theta_{1,2}}{V_1} \tag{2}$$

where

$D_{1,2}(A)$, $D_{1,2}(R)$ are the delay times for the thickness of the upper velocity (V_1) layer at point A and R respectively.

Similarly,

$$T_{AB} = D_{1,2}(A) + D_{1,2}(B) + \frac{A''B''}{V_2} \tag{3}$$

$$T_{RB} = D_{1,2}(R) + D_{1,2}(B) + \frac{R''B''}{V_2} \tag{4}$$

Using T_{A+} and T_{R+} of the T-D curve from shot points A and R, respectively, T_{B-} of T D curve from shot point B can be derived from the arrival and time of T_{AB} and T_{RB}.

Here in

$$T_{AB} = T_{AB} \tag{5}$$

$$T_{RB} = T_{BR} \tag{6}$$

Assuming the following relationship

$$DT = \frac{1}{2}(T_{AR} + T_{RB} - T_{AB}) \tag{7}$$

this equation can be rewritten by employing formulas (1) ~ (6) as

$$DT = \frac{1}{2}(T_{AR} + T_{RB} - T_{AB}) \tag{7}$$

$$= D_{1,2}(R) \tag{8}$$

when the T'_{AR}' so called "Hagitori" time, is represented by

$$T'_{AR} = T_{AR} - DT,$$

then from (8) formula

$$T'_{AR} = D_{1,2} + \frac{A''B''}{V_2} \tag{9}$$

The seismic velocity (V_2) is given by measuring the angle of the slope from these T-D curves.

However, undesirable factors are generally included in the results of analysis. They are:

i) The resolution of the recording system.

ii) Human made error in the reading of the arrival time.

iii) Assumption used for the analysis.

iv) Positioning errors of offshore surveys.

Among them, items ii) and iv) are considered to be the most likely errors in this analysis.

3-4-C Results of analysis

3-4-C-1 Volume of analysis

(1) The seismic velocity measuring survey of the main strata of Zonguldak area (on land).

This was performed to obtain some information for analysis of reflection and refraction methods.

The volume of the survey and analysis are as follows:

Surveying points	7 fields (No. 1 ~No. 7).
Length of surveying lines	20 ~ 35m x 7.
Sum of length	195m.

(2) The volume of analysis by refraction methods (offshore).

Table 35 shows the volume of analyzed lines, for the velocity distribution of the sea floor using reflection monitor records.

Total length possible to analyze refraction was 185.75 km.

3-4-C-2 Results of analysis.

(1) Velocity analysis of the main strata.

Usually, the velocity values of strata are obtained by sonic log (combined with γ ray or $\gamma - \gamma$ ray logs) and by well-shooting data at the boundaries of the main strata. But

Table 35 Analysed Lines of Seismic Refraction Method

LINE		SPREAD of ANALYSIS	LENGTH (km)	DIRECTION of LINE	SEA DEPTH (m)	REMARKS
JICA LINE	2	(S.P.–S.P.) 403–831	10.70	NE–SW	35–65	
	4	358–934	14.40	〃	60–110	
	6	780–964	4.60	〃	50–70	
	8	750–982	5.80	〃	60–150	
	101 (1, 2, 3)	-40–402	11.05	ENE–WSW	45–60	
	101 (3, 2, 1)	222–1,338	27.90	〃	40–70	
	103	0–280	7.00	〃	30–140	
		768–1,750	24.55	〃	25–200	
	105	712–870	3.95	〃	30–100	
	107	–	–			DEEP SEA DEPTH
	TOTAL		109.95			
MTA LINE	1	0–210	5.25	NE–SW	60–70	
	3	0–516	12.90	〃	55–90	
	5	790–950	4.00	〃	50–90	
	7	831–967	3.40	〃	60–80	
	9	0–176	4.40	〃	55–115	
	102	0–932	23.30	ENE–WSW	55–75	
	104	180–812	15.80	〃	55–100	
	106	–	–	〃	–	DEEP SEA DEPTH
	108	–	–	〃	–	〃
	A	226–290	1.60	NW–SE	55–200	
	B	46–138	2.30	〃	70–100	
	C	300–404	2.60	〃	50–80	
	D	240–290	1.25	〃	60–90	
	TOTAL		76.80			
G. TOTAL			186.75			

there was no well that performed a sonic log nor well-shooting in this area.

On the other hand, P-wave measurements on rock samples from the main strata were carried out by Hosono et. al. (1970).

The rock samples were only hard rocks like sandstone or limestone because of the difficulty in getting measurable samples. Also, this is pure rock data from the laboratory and it shows rather high velocities compared with that of strata in situ.

In measuring the velocity of the strata by the refraction method, approximately 30 m survey line was arranged at a possibly flat and freshly exposed area with a 5 m interval of receiving points and a seismic wave was generated by hitting an iron plate with a 20lb. hammer. The measurement was made with a Bison Stacker observing instrument (made in U.S.A.). The special feature of this instrument is to change the poor signal of the first arrival into a fair one.

Table 36 shows the locations of the surveying lines and the base rock velocity obtained from the measurements.

(2) Results of analysis by the refraction method (offshore).

Fig. 40 shows T-D curves and their velocity profiles.

Fig 41 and Fig. 42 show velocity distribution along the sea floor according to the results of the above mentioned analysis.

The outline of the analysis is as follow:

a) Depth of the sea at the area that can be analyzed
   25 ~ 100m (maximum 200m in some parts).

b) Area possible to analyze
   limited to 3 ~ 5km from the coast line.

c) Range of velocity value to be detected
   shows broad distribution covering 2.5 ~ 5.6 km/sec.

d) Summary of distribution of velocity
   i) 1 ~ 2km from the coast line over 3km/sec zone,
   ii) 2 ~ 4km from the coast line over 4km/sec zone,
   iii) between ii) and iv) 3 ~ 4km/sec zone with a width of 0.1 ~ 1km,
   iv) 2 ~ 5km from the coast line under 3.5km/sec zone.

Furthermore, within the high velocity zone (over 4km/sec), low velocity area (3.5km/

sec) are detected in various places.

3-4-D Consideration of results

3-4-D-1 Consideration of the results of velocity measurement of the main strata (on land area).

Results of the velocity survey of exposed rocks (Table 36) show rather low velocity compared to these deeper rocks.

This may be due to the looseness of the rock and the release of stress as they are crashed from blasting or folding, although they appear fresh.

The relative values of the velocity of different kinds of rocks seem to provide a good guide for presuming the kinds of rocks from the velocities which were obtained by analyzing the refraction and reflection, especially on the exposed rocks on the sea floor.

Table 36 Results of Velocity Survey of Base Rocks in Zonguldak Area

No	Location	Series and Rocks	Velocity	Line Length	Remarks
1	1 Km west of N.H.W. bridge, south side of cutting for Eregli N.H.W.	Aptian limestone	2.55 Km/sec	30 m	Velocity appears roller low because it exists near the surface and has some cracks filled with clay.
2	3 Km. southwest of Kozlu, west side of Begirmenagze, West side of cutting for N.H.W.	Vizean limestone (Sample No. 8111205-6	2.10 (Max 2.5)	30	ditto
3	West of Kaskoy, northside of the N.H.W., former site of cutting for power plant.	Lower Thronian glauconitic alternation formation (Upper part)	345	30	The velocity is fairly accurate because of very few weathering layers and the recent cutting for the power plant.
4	South side of the Gobu – Turkali N.H.W., 1 Km easy of Gobù.	Koniacian agglomerate	3.10	20	The rock body is somewhat weathered. Few intrusives in the cracks. A somewhat low velocity appears.
5	Near the river Filyos, west side of the N.H.W, 1 Km north of Comlekei, neighboring a fountain.	Kampanian biotile andesile	2.25	20	A columnar joint 5 ~ 6 cm square. Also, near the surface the side rather low velocity intrusive with clay.
6	On the Zongul dark-Ankara N.H.W 1.5km southeast of Zonguldak near Karaman.	Teritory sandy silt	1.35	35	A disseting of the topography and progressive, weathering near the surface causes low velocity.
7	Near the cross point of the new and old N.H.W, east side of the old N.H.W, 13.5 km southeast of Zonguldak.	Albian blue marl	1.75	30	The outside view of rock is fresh (slightly loose). Near the surface, many cracks and a rather low velocity.

Note N.H.W: National High Way

Fig. 43 shows the correction method of fresh rocks.

Assuming the fresh rock velocity is 5.0km/sec instead of 3.45km/sec for No.3 rock (upper part of the lower Turonian glauconitic alternation formation) and using this ratio for other rocks to distinguish them from exposed ones, corrected velocity values are also shown in Fig. 43.

Comparing the P-wave velocity obtained from this figure with that of a rock sample measured by Hosono (1970), some relationships between the two are presumed as follows:

a) In the case of limestone, the sample velocity ranges 6.5 ~ 7.0km/sec, but the base rock velocity is measured at only 3.0 ~ 3.7km/sec, perhaps from the effects of cracks.

b) In the case of the Koniacian agglomerate, they show nearly the same vales.

c) In the case of andesite, they also show nearly the same values.

d) In the case of sandstone, the sample velocity ranges between 2.1 and 3.9km/sec, but fresh base rock velocity is presumed at 2.0km/sec. It may be deduced that the westhering of the measured base rock has progressed. Then the true velocity will be the same as the sample velocity.

3-4-D-2 Consideration of the results of analysis by refraction. (offshore area). See Fig.42, 45 and 58.

(1) Seismic velocity of the results of analysis.

a) The possible analyzable sea area is that which is less than 100m in depth.

b) The analyzed velocity of the sea floor seems to be a rough value considering the accuracy of the analysis. Therefore, it is necessary to interpret the geology and geological instructures referring to the general distribution of velocity.

c) Low velocity areas in the high velocity zone suggest the existence of a fault or shear zone, or perhaps, in some cases, the variation of rock property (or facies).

d) The difference of velocity values at the cross point of survey lines will usually be interpreted as that the velocity is high when the survey line is in parallel with the crack direction and the velocity is low when the line is in a crossing direction with the crack.

e) In the results of the velocity survey of the exposed areas on land, pillow lava (glauconitic alternation formation) has the highest velocity. From the above, the over 4.4km/sec area, adjacent to the south side of the magnetic high anomaly axis, is presumed to correspond to the distribution of Pillow lava.

Assumption: The 3.45 km/sec of glauconite (maximum velocity of exposed rock) will be 5.0 km/sec of the usual velocity and the other exposed rock velocities are adjusted according to this rate.

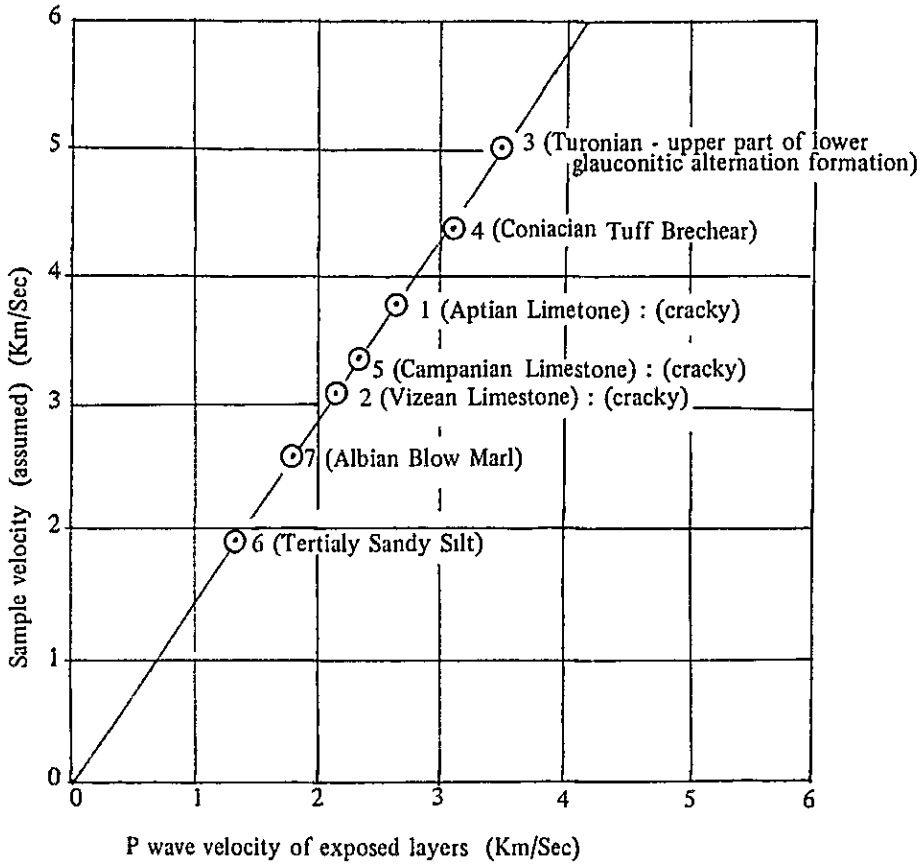

note 1; Exposed rock velocity and sample velocity are not at the same place.

Fig. 43 The relationship between exposed rack velocity and sample velocity (assumption).

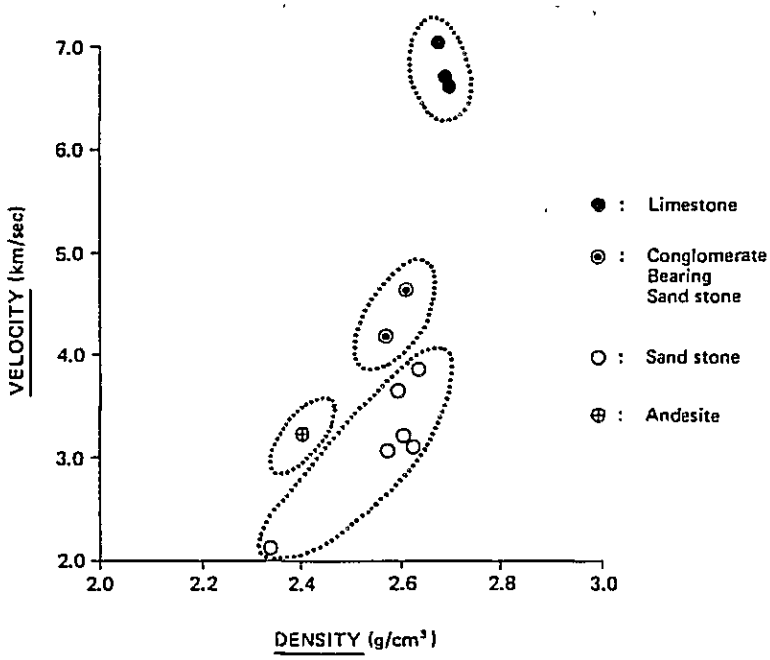

Fig. 44 Relation between Density and P-wave Velocity

(2) The relationship between the distribution of sea floor velocity and subsurface topography.

The boundary line of 3.5 km/sec, 2 ~ 4 km from tand parallel to the coast line, roughly corresponds to the boundary of the shelf to the steep dip region. This boundary also corresponds to the depth counter of - 100 m.

As for sea floor velocity, there exists a hard rock area with a high velocity on the shelf and a soft sediment layer with low velocity of less than 3.5 km/sec in the offshore area where the dip of subsurface topography becomes steep.

(3) The relationship between finding of the reflection and distribution of sea floor velocity.

a) The phantom horizon (for instance, the counter line of the "green" reflector in Fig. 36) has a relation parallel to the 3.5 km/sec velocity boundary and the - 100 m depth counter. It is presumed that a close connection exists among the sea floor topography, the distribution of sea floor velocity and the boundary of the phantom horizon in the offshore area up to 5 km from the coast.

b) In the offshore area on the refraction analysis, reflected waves are detected at some places. This may be caused by the new sediments with low velocity distribution in the upper part.

c) At the offshore of Kozul serisi (Kozlu coal bearing series) distributed in the Kozlu district, there is a low possibility to assume an existence of limestone because some reflector is detected at the west end of No.2 of the survey line.

(4) The relationship between the results of the gravity survey and the distribution of base rock velocity.

It is difficult to find a clear mutual relationship between the results of the gravity survey and the distribution of base rock velocity. But, on the residual gravity map, a sandwiched area with a high anomaly zone having a northeast-southwest direction along the coast line of Kilimli-Zonguldak-Iliku, and a low anomaly zone about 3.5 ~ 4.0 km from and parallel to the coast line, as well as an area between the above high anomaly and a low anomaly 3 ~ 4 km to the south in parallel to the former, coincide with an over 4 km/sec high velocity areas and seem to reflect the geological structure of the shallow area distributed with hard rock.

Also the axis of low anomaly area at the offshore area roughly coincides with each contour of -100 m in depth, 3.5 km/sec of velocity and reflection time of 0.5 sec.

This seems to suggest the geological structure of this offshore area.

(5) The relationship between the results of the magnetic survey and the distribution of sea floor velocity.

From the fact that land areas sandwiched with magnetic high and low anomaly axes closely correspond to the distribution of agglomerate, offshore areas sandwiched between the two axes are also attributed to the distribution of them.

Also, from the distribution of sea floor velocity, an area sandwiched by a 4.0 km/sec boundary on the northern half of the offshore of this agglomerate zone and the low anomaly axis is thought to be a latent distribution zone of andesite.

(6) The relationship between geology and the distribution of sea floor velocity.

This relationship has been already described but, in this case, other geological conditions derived from survey data are shown as follows:

a) The velocity zone of under 4.0 km/sec at the edge of the shelf and the offshore area from the 3.5 km/sec velocity boundary along the edge of the continental shelf are believed to be soft sediments of the Tertiary.

This boundary has a good correspondence with the truncated part of a shallow reflected layer.

Some part of the under 3.5 km/sec zone may be considered to be a sheared zone caused by a fault.

The area which is sandwiched by presumed limestone and agglomerate, is possibly distributed with blue marl, glauconitic sandstone, Velibey sandstone, and marly flish of the Tertiary.

b) As for the distribution of limestone along the coast line, the fact that the velocity of limestone on land, appears to be lower than the fresh sample velocity due to cracks seems to indicate a low possibility of the existence of limestone in the high velocity areas of over 4.3 km/sec.

Assuming that the limestone is distributed in the area of 4.3 km/sec, some part of them must belong to the high manetic anomaly area, which contradicts the property of the non-magnetism of limestone. On the bases of this idea, the extended area of limestone offshore has been inferred from the distribution on land.

3-5 Interpretation of Gravity Survey

3-5-A Purpose

The purpose of the interpretation is to serve as a supplementary measure in analyzing the geological features of this region by means of quantitative and qualitative interpretation methods applied to all the data acquired from both on land and offshore regions.

3-5-B Method of interpretation

For the offshore survey, especially in the near shore region, to analyze the underground geological features, it is necessary to interpret this data in close connection with the results of the on land geological survey. Then, a Bouguer anomaly map (Fig. 46) of this region was made as the foundamental map of the interpretation of gravity survey by compiling both offshore and on land data. However, there was a big difference in the density value of rocks sampled for elevation correction between the offshore area (2.67) and the on land area (2.40). In order to avoid a possible confusion in the interpretation by using different density values in a limited area, the value obtained on land, considered to be more reasonable of the two, was used as a common value both on land and offshore area, and the offshore data were recalculated accordingly.

On the other hand, many fluctuations were recognized in the measured values on each survey line, probably caused by instrument errors. So after studying the tendency of the gravity gradient on each line and making the intersection control, the Bouguer anomaly map has been prepared.

3-5-B-1 Qualitative interpretation

Presuming that with only a Bougher anomaly map, it would be difficult to correlate with a geological map, the residual values have been calculated by means of a running average method (Hagiwara's method) as same as the experimental operation. This method is one of the band pass filtering procedures which was reformed from Seya's method.

The procedure of this method is as follows. First, a grid system is drawn on the Bougher anomaly map with an adequate spacing, approximately the same dimension as the depth to be investigated. Then, the Bougher gravity value at every grid point is read off for the preparation of the following:

– Separation of high frequency component (Noise Structure)

$$G_N\ (m, n) = g\ (m, n) - \frac{\sum_{i=m-1}^{m+1} \sum_{j=n-1}^{n+1} g\ (i, j)}{9}$$

– Separation of intermediate frequency component (Normal Structure)

$$G_M\ (m, n) = \frac{\sum_{i=m-1}^{m+1} \sum_{j=n-1}^{n+1} g\ (i, j)}{9} - \frac{\sum_{i=m-3}^{m+3} \sum_{j=n-3}^{n+3} g\ (i, j)}{49}$$

– Separation of low frequency component (Regional Structure)

$$G_R\ (m, n) = \frac{\sum_{i=m-3}^{m+3} \sum_{j=n-3}^{n+3} g\ (i, j)}{49} - \frac{\sum_{i=m-7}^{m+7} \sum_{j=n-7}^{n+7} g\ (i, j)}{225}$$

where g(i,j) is a reading of the Bougher anomaly value at the grid point, and m,n show grid positions. Three kinds of Residual Gravity maps are obtained through figuring the isolalue contour using these calculated values with these formulas.

In this analysis, efforts have been made to obtain a more detailed geological structure, by narrowing the interval of grid lines from 1 km. of the experimental operation to 0.5 km. and also by adopting the Regional and Normal Structure maps (Fig. 47 & 48) against the Normal Structure map only. These calculations were performed by using the M.T.A. computer system (General Purpose Interdata 8/32 computer system).

3-5-B-2 Quantitative Interpretation

The same curve matching method with a two dimenional infinite horizontal sheet was used as same as the experimental operation. In this method, the gravity effect at a surface point (P) is calculated assuming a subsurface model which is composed of several horizontally extended infinite sheets as shown in Fig. 49.

Gravity ($g_G(P)$) at the point (P) is –

$$g_G(P) = 2 \cdot G \cdot \theta \cdot \vartheta \cdot \delta$$

where G : Constant universal gravitation (6.67×10^{-8} dyne $cm^2 \cdot g^{-2}$)

θ : Included angle at P between both ends of the sheet (degree)

ϑ : Density (g/cm^3)

δ : Thickness of sheet (km.)

A total gravity effect caused by the overall subsurface model at point P is thus calculated by summing up the individual effect of each sheet.

If mgal is used as a gravity unit, it is given as

$$g_G(P) = 0.2328 \cdot \theta \cdot \vartheta \cdot \delta$$

To obtain a simulated subsurface structure, this calculation is carried out for a considerable interval along the X-axis changing the value of θ, and until the calculated profile is closely fitted to the observed one. In this study, this calculation was applied to six profiles, of which four profiles were parallel to the seismic survey lines, A, B, C and D, running nearly perpendicular to the coast and two profiles were along the geological profiles being parallel to the lines A, B, C and D. A thickness of 0.25 km. was applied for the horizontal sheet and a value of 0.27 was adopted as the difference of density. In addition, as a reference for the interpretation of gravity survey result, the density value of rocks collected on land and measured at E.K.I. laboratory have been used as well as those in the Hosono's report used in the experimental operation. (See Table 37)

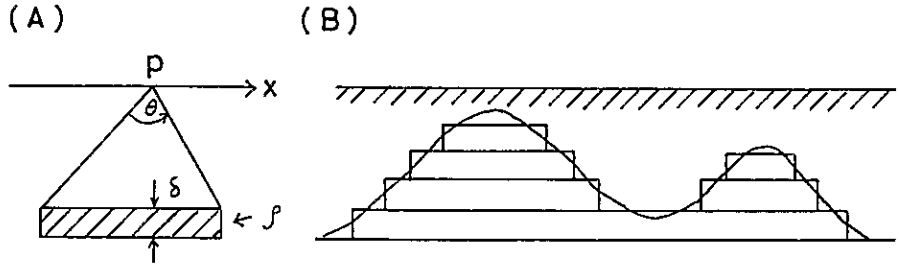

Fig. 49 Two-dimentional Horizontal Plate Model

Table 37 Stratigraphy and Physical Properties of Rocks in Zonguldak District

System	Series	Formation	Symbol (1)	Thickness	Density		Susceptibility S.I unit x 10^{-3}			
					Hosono (2)	E·K·I (3)	Bōjō et al. (4)	Hosono (2)	Inoue (5)	M·T·A (6)
Tertiary	Eocene ~ Paleocene	Marl & Filish F.	PE	—			16			
Cretaceous	Maestrichtian S.	Chalky Marl F.	Krame	500m±		2.55			0.02~0.45	
	Campanian S	Andesite F	An	130m±		2.46	21.3		14.1~16.4	
		Marly Alternation F	Krka	480m±					silt 0.21 mud- 0.07 stone ~0.11	
	Santonian ~ Coniacian S.	Upper Agglomerate F	Ag	380m±	2.39	2.55	29~55	73	25.1~62.1 (Max. 81.1)	3.77~10.8
		Lower Agglomerate F		250m±					Upper 28.3~34.3 Lower 17.1~25.1	
	Turonian S	Thin bed Marl F	Krtu	0~50m					0.05	
		Upper Glauconitic Alternation F	Tup	170m±		2.36 ~ 2.51	10~21		0.91~6.3 (Max 14.1)	0.63~6.28
		Middle Glauconitic Alternation F		200m±					3.78~4.56	
		Lower Glauconitic Alternation F		250m±					0.10~5.71 (Max 10.5)	
	Senomanian S	Upper Flish F.	Krse	100m±					0.05~0.07	
		Blue Marl F	BM	130m±					0.15	0.63~0.88
	Albian ~ Aptian S	Calcalious Sandstone F	Kral	200m±					0.05~0.07	
		Marly Silt Stone F	Vs	200m±					0.05~0.11	
		Lower Marly Flish F	Kraps	450m±		2.63	0.24		0.05~0.07	
		Aption Limestone F.	Apl	200m±	2.69	2.71	0.2~0.5	0.3	0.00	0 ~ 0.8
	Barremian S	Incuvez F	Krba	30m±					0.02~0.09	
		Barremian Limestone F	Bal	200m±		2.67 ~ 2.70	0		0.00~0.02	
Carboniferous	Westfalian S	Karadon Conglomerate F	Ka	300m±	2.32 ~ 2.56		0.25	0.6	0.07~0.11	0.6
		Kozlu Coalbearing F	Kw	700m±	2.56 ~ 2.61				0.12~0.22	
	Namurian S	Fine~Medium Sandstone F.	Na		2.62		0.8			0 ~ 1.0
	Visean	Limestone F	Ve				4.4			
Devonian			Dev							

Note

(1) Symbols used in the Geological Profile (compiled by Mr. Bōjō)

(2) Hosono M et al (1970) Report on Geophysical Prospecting of Offshore Area of Kozlu Coal Mine, Zonguldak Coal Field, Nittets Mining Conultants Co, Ltd.

(3) Measured By E K I members (Sampled by J.I.C.A team) masured with pignometer

(4) Bōjō T et al (1970) Technical Cooperation Report on Exploration of Offshore Area of Zonguldak Coal Fied, Turkey

(5) Measured by Inoue (Chief of J.I.C.A team)

(6) Measured by M.T.A members

3-5-C Results of interpretation

3-5-C-1 Quantitative interpretation

a) Bouguer anomaly map

The major tendency dominating in the almost entire region is as follows:

a-1) A gravitational anticline running east-northeast to west-southwest direction and having an apex at about 7 km. southeast of Zonguldak.

a-2) A steep descending gradient which is nearly parallel to the above-mentioned gravitational anticline, starting from 0.5 to 1.5 km. offshore of Zonguldak coast and having an extent of 2.5 to 4.0 km. long.

a-3) Another steep descending gradient on land at the symmetrically opposite side of the above-mentioned gravitational anticline.

Among others, several somewhat remarkable anomalies, such as a low one at the southwest part of this region and high and low ones at offshore area, were recognized.

b) Regional gravity map (Regional Structure)

b-1) On land, a high anomaly zone, having its center at Uzunburum, extends to the eastwards and connects with the remarkable high anomaly zone to the east of this region. There is a low anomaly zone directly adjacent to the above-mentioned remarkable high anomaly zone on its southeastern side.

b-2) Near the coast, a high anomaly zone existing between Kilmi and Catalagzi concontinues to another high anomaly zone 2 km. west from Zonguldak. Furthermore, a high anomaly zone having its center at Iliksu, was shown along the coast line. A low anomaly zone being sandwiched between the above-mentioned two high anomaly zones extends to the eastwards from Kozlu.

b-3) At offshore region, there is a very long low anomaly zone, which has an axial line almost parallel to the coast line and be aparted 3 to 5 km. from the coast. This low anomaly zone changes the axis to the northeast-southwest at the offshore area of Kozlu.

c) Residual gravity map (Normal Structure) (Fig. 47)

In general, the remarkable anomaly area in the Regional Structure map are fractionized and also some of their center positions change slightly from the Regional Structure map.

c-1) On land, the high anomaly area recognized near the coastal line of Iliksu in the Regional Structure map, continues to the remarkable high anomaly area on the

southeast side of the region. But this high anomaly zone slips cut somewhat from that in the Regional Structure map and be fractionized. The low anomaly area adjacent to the remarkable anomaly area is also reduced in its size.

c-2) Near the coast line, the high anomaly area starting from nearly Kilimli shows a tendency to extend toward further to the west than that observed in the Regional Structure map. The high anomaly area at Iliksu is fractionized. Furthermore a low anomaly area at Kirencik is apparent.

c-3) In the offshore region, the low anomaly area, having the same axis as shown in the Regional Structure map, extends and changes its direction of axis at offshore area of Kozlu.

d) Gravity profile (Fig. 51 – 56)

For each profile, a steep dip is calculated at the offshore section.

d-1) A-A' profile corresponds to the A line of the seismic survey and its extention on land area. In this profile, a steep dip starting at 0.4 km. from the coast line is remarkable. In addition, a steep dip is also inferred on land. On the northwest side of the offshore section, the gravity basement appears rather shallow.

d-2) B-B' profile is made along B line and extended on land. In this profile, a steep dip appears starting at 1.5 km. from the coastal line and be infered to have a tendency to be somewhat uplifted further offshore. On land, the same as in A-A' profile, a steep dip to the southeast side is infered.

d-3) C-C' profile is made along C line and extended on land. A steep dip appears at 1.5 km. from the coast line and becomes near 70° at around 3 km.

d-4) D-D' profile is made along D line and extended on land. In this profile, a steep dip starts at 0.6 km. and reaches its deepest point at 3 km. At 4 – 6 km. it is uplifted steeply.

d-5) E-6 profile is made between the B-B' and C-C' profiles and parallel to them. In this profile, a steep dip appears at 1 km. and tends to be uplifted at 5 km.

d-6) E-8 profile is made between the C-C' and D-D' profiles and parallel to them. In this profile, a steep dip appears at 1 km. and is uplifted at 5 km.

3-5-D Consideration of offshore gravity survey

Some consideration has been made to presume the geological structure by refering the results of the interpretation of gravity survey and the geological studies on the land area.

With Table 37, thedensities of rocks distributed in this region have little difference except those of low density rocks belong to the Tertiary and the upper Cretaceous age. It also

seems that the limestone of the lower Cretacenous has a rather high density compared with coal bearing formations of the upper Carboniferous.

3-5-D-1 Qualitative interpretation

a) Bouguer anomaly map

As mentioned above, there are no remarkable differences among the densities of rocks. So it is difficult to find a correlation between the geological structure and the Bouguer anomaly maps. Only the steep gradient of isogal lines recognized on the southeastern section of this map correlates to the large fault dipping to the south, and the low gravity area on its southeast is identical with the distribution of sandstone of the Tertiary Furthermore, in the high gravity area of the central part, it is presumed that each stratum of the Palaeozoic is present in a relatively shallow sequence, in view of the Cretaceous formations showing a relatively gentle syncline structure.

On the basis of the above results, offshore geological structure are inferred. For example, a deep gradient toward the northeast and its contour parallel to the coast line, seems to indicate a steep dip and/or fault in this position. The bending of the direction of this steep dip observed on the west of Zonguldak is presumably due to an existence of another fault which had possibly shifted the above-mentioned steep dip or the fault horizontally.

Also, a broad low gravity area farther apart from the coast line infers the presence of Tertiary formation.

b) Residual gravity map (Regional structure)

i) On land, a high anomaly area expanding from east to west with its cneter at Uzunburun, covers a part of the distribution of the Carboniferous Visean limestone. But as this distribution is also seen near the low anomaly area, it is possible to indicate that the weathering may have progressed partially.

This high anomaly area also extends further east and connects with a remarkable high anomaly area. The latest is identical with the Visean limestone of the Carboniferous and the Devonian limestone.

The low anomaly area in contact with this high anomaly area on its southwest is identical with sandstone of the Tertiary. The low anomaly area at 3 km south of Catalagzi, where limestones of the Barremian and the Aptian area distributed, corresponds to the location of a synclinal structure on the geological map, and

also it seems to be related with the rate of weathering. The location of the large fault on the southwest mentioned in the section of Bouguer anomaly map roughly agrees with the "0" line of the contour.

ii) Near the coast line, a high anomaly area which extends from Catalagzi to Zonguldak is identical with the exposure of linestone of the Aptian and the Barremian. A high anomaly area extending offshore to the west of Zonguldak is also presumed to be a distribution of these limestones, as is the high anomaly area which extends from Kozlu to 4 km southwest of Iliksu.

The low anomaly area 2 km east from Kozlu corresponds to the area of the distribution of the Westphalian coal bearing formation. Therefore, it indicates that the density of this coal bearing formation is lower than that of limestone of the Cretaceous and the Carboniferous. Also, as this low anomaly area varies the direction of the axis of the nearby high anomaly, it is presumed to indicate the presence of a fault.

iii) Considering the offshore region on the basis of the correlations mentioned in b)-ii), the steep gradient parallel to the coast line seems to indicate a fault or steep dip centering around the "0" line. The low anomaly area in contact with this steep gradient is probably of the Tertiary origin. On the other hand, the bending of "0" line in the vicinity of Kozlu is believed to represent another fault.

c) Residual gravity map (Normal structure)

As mentioned before, anomaly areas are fractionalized as compared with the Regional gravity map.

i) On land, the high anomaly area with its center at Uzunburun extends toward the east although it is fractionalized. This area is identical with a parts of the Visean limestone. But a relatively high anomaly area at 6 km south of Zonguldak is identical with a calcareous sandstone formation of the Albian and it is also present on the Regional Structure map. It is possible then, that this formation thickens locally. The high and low anomalies of the southeast side of this region area, as on the Regional Structure map, identical with distributions of limestone formations of the Visean and the Devonian, and the formations of the Tertiary respectively. Furthermore, the fault between them is observed, the same as on the Regional Structure map.

ii) Near the coast line, the high anomaly area on the west side of Zonguldak extending east-northeast, is identical with the exposure of limestone formations of the

Aptian and the Barremian. There is also an evidence that this high anomaly area extends off west of Zonguldak to the west-northwest, just as on the Regional Structure map. Furthermore, a fractionalized high anomaly area having its center at Iliksu seems to have some relation with the distribution of the Aptian and Barremian limestone. A low anomaly having its center at Kirencik, is identical with the distribution of an upper formations of the cenomanian flysh. Therefore, it is assumed that formations older than the Senomanian are somewhat deeper.

iii) Considering the offshore region on the basis of the findings in c)-i) and c)-ii), a steep dip or fault must be present between the high anomaly on the coast line and the low one very close to it on its offshore side. A distribution of the Tertiary formations is presumed to present in the low anomaly area. The fault believed to be present off Kozlu is thought to be perpendicular to the coast line.

3-5-D-2 Quantitative interpretation

On the land portion of each profile, the correlation between the results of two-dimensional horizontal analysis and the geological profile appears to show that the boundary between rocks of different density corresponds to the upper horizon of the Albian. This interpretation is not contrary to the results of density measurements. (Table 37)

However, the central part of the land area, where limestone formations of the lower Cretaceous are erroded, shows a relatively low gravity value, due apparently to the relatively low densities of rocks of the Karadon and Kozlu formations. The fault position on the land region is shown on the A-A' and B-B' profiles, but it is not so evident on the other profiles.

Some consideration for the offshore part of the each profile has been made based on these findings. However, the geological profile of the offshore area has been inferred only from the probable thickness and the dips of each formation observed in land and has not been confirmed with the results of dredging of drilling. This must be corrected successively with the results of further surveys and underground drillings.

a) At the shallow part of the A-A' profile, the boundary of gravity is almost identical with that of the boundary of the formation. This boundary reaches 3,000 m in depth about 4 km from the coast and then levels off until 8 km, after which it uplifts somewhat. In this profile, it cannot be concluded that this steep dip is accompanied by a fault.

b) At the shallow part of the B-B' profile, both boundaries are almost identical with each other. This boundary, as with the A-A' profile, becomes deeper until 9 km from the coast line where it reaches a depth of 5,000 m. A fault is inferred from its shape near

2.5 km.

c) The shallow part of the C-C' profile shows a different phase of the geological profile. That is on geological profile, calcareous sandstone of the Albian outcrops at 1 km from the coast line, but on this profile, a high anomaly area is recognized extending over 2 km distant from the coast. This may be reasonably explained by the influence of formations of the Aptian and the Barremian limestone which lay offshore near this profile.

d) As to the shallow part of the D-D' profile, it is identical with the geological profile, but shows a very deep valley which is calculated like a graben. It reaches 7,000 m in depth at 3 – 4 km from the coast. This probably indicates the presence of rather low density rocks (including a fractured zone).

f) E-8 profile seems to reveal a fault at 2 km, and appears to become nearly flat at 3 km.

3-5-D-3 Summary of the interpretation of Gravity Survey

As is almost evident on the correlation between the geological profile and each gravity profile, the boundary of the density difference seems to be present at the level of the middle to lower Cretaceous, that is, between upper calcareous sandstone of the upper Albian and limestone of the upper Aptian. Therefore, from the viewpoint of the gravity survey result, it seems more suitable to regard it as the upper albian. The Bouguer anomaly map is thus assumed to be closely correlated with the depth map of one of those formations. The high anomaly areas of the Residual gravity maps, both Regional Structure and Normal Structure, are closely related to distributions of limestone. Also, the distribution of coal bearing formations of the Carboniferous show rather low anomalies compared to their neighbors. It is explained that there is some relation between the gravitational basin structure and the distribution of coal mines, as pointed out at the experimental operation.

In the cases where these formations are covered with the upper formations, they are interpreted to be included in the layers with the density 2.67.

3-6 Interpretation of Magnetic Survey

3-6-A Purpose

The purpose of this interpretation is the same as that of the gravity survey, that is, to serve as a supplementary measure in analyzing the geological features by means of qualitative and quantitative interpretation applied to all data aquired from both land and offshore regions.

3-6-B Method of interpretation

As with the gravity survey, it is necessary to interpret the offshore data in close eonnection with the results of the on land surface geological survey. The results of the total magnetic intencity measurement of the land surface survey were processed by upward continuation and then be correlated and checked with those of both the offshore and airborn on land surveys. Various methods have been developed for that procedure. This time, the calculation was performed by M.T.A. members using Peter's method, the method used most commonly by them.

In consequence of that calculation, no discrepancies were found between the results of the land, offshore and airborne surveys. A magnetic anomaly map (Fig. 50) of this region was then made and presented as the fundamental map for interpretation. In this case no big difference in the measured values was found at any intersection.

3-6-B-1 Qualitative interpretation

As it was obvious that the magnetic anomaly map had a good correlation with the geological map at the time of experimental operation, they were used for qualitative interpretation as they were, and a I.G.R.F. (International Geomagnetic Reference Field) correction was not performed.

3-6-B-2 Quantitative interpretation·

At some places on each gravitational profile, a three dimentional interpretation (Tsu's method) was applied as it was in the experimental operation. This method is basically used, assuming the first approximation of the subsurface magnetic body. Then the calculation is carried out changing the parameters (width and depth) of the prism model until the best curve has been obtained.

In this case, they were calculated by the M.T.A. computer system.

The basic formula is given as follows:

$$\Delta T(x, y, H) = J \cdot G(x, y, z)$$

$$G(x, y, z) = \left[\frac{\alpha_{23}}{2} \log \left(\frac{\gamma_0 - \alpha_1}{\gamma_0 + \alpha_1} \right) + \frac{\alpha_{13}}{2} \log \left(\frac{\gamma_0 - \beta_1}{\gamma_0 + \beta_1} \right) - \frac{\alpha_{121}}{2} \log (\gamma_0 + H) \right.$$

$$- \ell L \tan^{-1} \left(\frac{\alpha_1 \beta_1}{\gamma_0^2 + \gamma_0 H - \beta_1^2} \right) - m M \tan^{-1} \left(\frac{\alpha_1 \beta_1}{\gamma_0^2 + \gamma_0 H - \alpha_1^2} \right)$$

$$\left. + n N \tan^{-1} \left(\frac{\alpha_1 \beta_1}{\gamma_0 H} \right) \right] \left| \frac{\alpha\mu}{\alpha\ell} \right| \frac{\beta\mu}{\beta\ell}$$

where

$\alpha_1 = \alpha - x$, $\beta_1 = \beta - y$, $\alpha_u = L_x - x$, $\alpha_\ell = -L_x - x$,

$\beta_u = L_y - y$, $\beta_\ell = -L_y - y$, $\gamma_0^2 = (\alpha - x)^2 + (\beta - y)^2 + H^2$

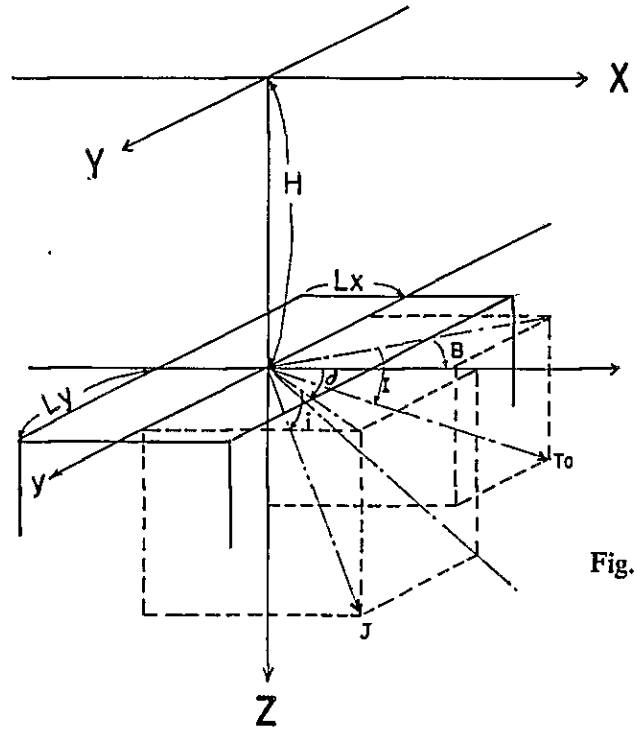

Fig. 57 Principle of Magnetic Analysis on Three-dimensional Prism Model

However, there were some discrepancies between the model and the geological features as the dips were so evident. Recalculations were made in those places where an anomaly was regarded as the cause using Koulomzine's method of a two-dimensional magnetic body. This method is not so different in its basic principle except it presumes the magnetic body directly from the magnetic distribution. These results are shown on each gravity profile.

Furthermore, the susceptibility of rocks on this region has been measured by many people. The results of these measurements are also shown in Table 37.

3-6-C Results of interpretation

3-6-C-1 Qualitative interpretation

As a general tendency, on land area except in anomaly zones, magnetic intensities increase at the rate of 30–50 gamma/km toward the coast.

a) On land, a small anomaly area, recognized near the coast line on the east-northeast side of this region, continues to the wide anomaly area in the south bending the direction of the axis of the anomaly. The center lines of the maximum and minimum anomalies cross at 3 km southeast of Türkali. On the southern part of this region, the center of the minimum anomaly runs along the coast. In the south-western part, a minimum

anomaly zone running from east to west is recognized.

b) Near the coast line, only the small anomaly area mentioned above, is distributed perpendicular to the coast line. In addition, near Zonguldak and Kozlu, Iliksu and also Kandilli, the intervals of isogamma lines seem rather large compared to their neighbours.

c) Offshore, maximum magnetic anomalies which have their centers 1 km from the coast line off Gobu, 3 km off Zonguldak, and 2 km off Kozlu and Kirencik, are recognized.

3-6-C-2 Quantitative interpretation

Each profile shows anomalous distribution caused by two or three kinds of rocks having high susceptibility. At this time, calculations were made by picking up only the main anomaly distribution. But as they were calculated on an assumption that they are uniformly magnetized, the depth, width, and dip of magnetic bodies should be regarded as a tentative reference.

a) A-A' profile (Fig. 51)

On land, a wide magnetic body is shown on the south-eastern side. Probably this may be caused by a complex of magnetic bodies. But they could not be separated as they are too small in their variation.

Offshore, the main magnetic body is assumed by calculation at 3 km from the coast, while a small one with low susceptibility is also shown at about 0.4—0.5 km from the coast.

b) B-B' profile (Fig. 52)

On land, a broad magnetic body is inferred by calculation on the southeastern side and another one with low susceptibility is inferred adjacent to the main body on its left side (northwesterly).

Offshore, a main body, having its center at 3.5 km from the coast line, is assumed by calculation. Another one with low susceptibility alos seems to be present at 2.0 km from the coast.

(c) C-C' profile

On land, there is a broad magnetic anomaly at the southeast end . On the left side of this main body, there is a small magnetic body with low magnetic susceptibility. On the other side of the main body, there is a sign of existence of a magnetic body which may have a similar scale magnetic susceptibility with the main body.

Offshore, a main body has been assumed by calculation and there are apparent signs of

existences of other bodies on both sides of it.

d) D-D' profile (Fig. 54)

On land, no apparent variation is recognized.

Offshore, a main body has been inferred by computation with its center at 2 km from the coast line. Another one was observed between the main body and the coast.

e) E-6 profile (Fig. 55)

On land, a broad anomaly area is shown on the southeast end. It has a main magnetic body accompanied by another one with low susceptibility on its left side.

Offshore, a main body having a center at about 2.5 km from the coast and another one with low susceptibility to its right side are shown.

f) E-8 profile (Fig. 56)

On land, a sign of a magnetic body on the southeast end has been shown.

Offshore, a main body has been infered so as to have its center at 2 km off the coast and another one with low susceptibility is also assumed on its right side.

3-6-D Consideration of magnetic survey

Some consideration has been made to presume the offshore geological structure based on the study of the correlation between the results of surface geological studies and the interpretation of magnetic surveys using susceptibility as a reference.

3-6-D-1 Qualitative interpretation (Fig. 50)

The general tendency of the Magnetic anomaly map could be eliminated using I.G.R.F. correction. (But in this case it was not performed).

a) On land

The anomaly area having the maximum and minimum ones, as shown on the coast line of the northeast corner, is identical with the distribution of tuff breccia of the Santonian and/or the Coniacian of the Cretaceous. The disturbance of the isogamme line near this area coincides with the distribution of a glauconitic alternation formation. This anomaly area varies the direction of the center lines of maximum and minimum values and, especially 3 km southeast from Turkey, both center lines seem to cross each other. These center lines bend their directions variously and extend from east to south. This anomaly area also corresponds to the distribution of tuff breccia. The crossing of the center lines and the inversion due to them are presumed from the relation of the dip of the magnetic body and the inclination of the magnetic field

of the earth. But, as andesite is in contact with this anomaly area on its east and affects the anomaly by tuff breccia, it is difficult to separate these anomalies except near the coast line.

The distribution of andesite along the large fault (mentioned in the gravity survey) running from northeast to southwest on the southeast side of the geological map, is presented as only a small anomaly area on the Magnetic anomaly map. The anomaly area extending at the south side of this map is caused by andesite, judging from the geological map. Near this anomaly area to the north, a tuff brecia formation is distributed. This distribution extends to the southwest side, but it is only a broad anomaly area without showing great anomalous value, except partly on the southwestern margin. But the difference between andesite and agglomerate is not so evident. From this consideration, it can be concluded that rocks which cause magnetic anomalies are mainly tuff breccia and andesite, followed by glauconitic alternation.

Also, the susceptibility of tuff breccia seems to be higher or the same as that of andesite from the north to the southeast side of this area, but it seems to be rather low on the south side.

b) Offshore

The large anomaly area distributed parallel to the coast line from northeast to southwest, is interpreted to be caused by tuff beccia, presumed from tis distribution on land, especially near the northeast side of the coast line. But small anomaly areas, scattered on the shore side of the above big anomaly are interpreted to be caused by glauconitic alternation. And others, such as the areas of the relatively wide interval of the isogamme contour near Zonguldak and Kozlu, as well as near Iliksu coincide with the distribution area of the Aptian and Barremian limestone.

The west end Kozlu, where the center line of maximum magnetic anomaly changes its direction, seems to show the pressure of a fault.

3-6-D-2 Quantitative interpretation

This calculation has been done only to find the effects of the main magnetic bodies on smoothing the anomaly curve. On the calculated results of the land region, dips and center positions do not contradict the geological profile.

a) A-A' profile (Fig. 51)

On land, the anomaly range corresponds to the position of a complex tuff breccia and andesite, but it is too small in variation to be calculated.

Offshore, the calculated main body is correlated with agglomerate on the geological profile. A small one whose center is 0.4 – 0.5 km from the coast, is assumed to be a glauconitic alternation formation.

b) B-B' profile (Fig. 52)

On land, the main magnetic body is correlated to andesite. Tuff breccia also has large effect on the magnetic anomaly curve, but the two cannot be separated from each other.

Offshore, the main magnetic body which has a center at 3.5 km from the coast line, is presumed to be tuff breccia. A small anomaly area 2 km off the coast seems to correlate with glauconitic alternation formation.

c) C-C' profile (Fig. 53)

On land, the location of the calculated body is identical with the distribution of an andesite formation. On the left side of this location, a tuff breccia formation cause a small magnetic anomaly, and on the right side, another andesite formation seemingly disturbs the shape of the anomaly curve caused by the main andesite formation.

Offshore, the main calculated body is inferred to be tuff breccia, but the magnetic bodies causing disturbances to the anomaly curve on both sides of the main body are inferred to be andesite on the offshore side and glauconitic alternation on the coast side.

d) D-D' profile (Fig. 54)

On land, the zone of small variation on the anomaly curve coincides with the distribution of tuff breccia, but it is too small to calculate.

Offshore, the calculated main body is presumed to be tuff breccia, and the small one on the shore side seems to be correlated with glauconitic alternation.

e) E-6 profile (Fig. 55)

On land, the calculated body is considered to be a complex of andesite and a tuff breccia formations, but they cannot be separated because the variation is irregular.

Offshore, the calculated body is considered to be tuff breccia formation, and a small anomaly zone on the coastal side seems to be a glauconitic alternation formation.

f) E-8 profile (Fig. 56)

On land, a sign of an anomaly corresponds to tuff breccia.

Offshore, the main calculated body is presumed to be a tuff breccia formation, and a

a small one near the shore is considered to be a glauconitic alternation formation.

3-6-D-3 Summary of interpretation of magnetic survey

A correlation has been made between the results of the interpretation of the magnetic survey and the geological map and its profiles.

From these results, it may be concluded that there are three kinds of rocks which cause anomalies in this region. They are : tuff breccia, andesite, and glauconitic alternation formations.

Among these rocks, the susceptibility of glauconitic alternation formations is smaller than the first two and only disturbs the anomaly curve.

Andesite is in existence along the large fault on the south and southeast sides of this region, and tuff breccia contacts with it on the south side.

But on the northeast side of this region, both of them are clearly separated on the geological map, and the anomaly caused by tuff breccia, with the center axes of maximum and minimum values crossing at 3 km southeast from Türkali, appears to continue to the large magnetic anomaly zone offshore. Thus, the magnetic body of the latter area is recognized as tuff breccia.

As all the rocks causing magnetic anomalies are those of the upper Cretaceous, the Carboniferous coal bearing formations are considered to be covered with them.

Together, they form a large anticlinal structure, and the Cretaceous formations also have some thickness. Therefore, at this time, the minable areas are limited to the inner area surrounded by the magnetic bodies.

VI. OVERALL INTERPRETATION AND RECOMMENDATIONS

[illegible]

VI. OVERALL INTERPRETATION AND RECOMMENDATIONS

1. OVERALL INTERPRETATION

1-1 Geological Structure in the Offshore Area

(1) The geological survey revealed that the Cretaceous formations were developed around the anticlinal structures, which are the Amurtçuk Anticline, Kozlu-Karadon Anticline, and Amasura Anticline from the west running ENE-WSW direction parallel to the coast around Zonguldak City. (Figs. 6 & 7).

(2) It is considered from the geophysical survey that the north wing of the anticline is located offshore as discussed below.

(a) The seismic reflection from the possible upper Cretaceous formation indicates that the formation dips northwards gently near the shore and dips steeply offshore 3 – 4 km away from the coast (Fig. 37).

(b) Velocity less than 4.0 – 3.5 km/sec. at the sea floor off the continental margin more than 3 – 4 km away from the coast suggests the occurrence of soft sediments. (Fig. 42)

Low velocity in the order of 2 km/sec. is obtained by the reflection velocity analysis. The reflection pattern on the seismic section also suggests the occurrence of soft sediments. (Fig. 33)

(c) On the contrary, hard formations more than 4 km/sec. velocity occur landward. (Table 36, Figs. 42, 43, & 44)

(d) The bougher anomaly contours (Fig. 46) seem to be related to the depth contours of the Middle – Lower Cretaceous, i.e. the top of the Albian calcareous sandstone or Aptian limestone. A positive gravity anomaly defined on the residual gravity map (Figs. 47 & 48) seems to be related to the Lower Cretaceous and/or Palaeozoic limestones. The low gravity obtained in the offshore possibly coincides with the Tertiary sediments.

1-2 Geology and Structures in the Anticlinal Area Offshore Along the Coast

(1) Distribution of limestone

(a) Concerning the offshore extention of the onshore limestone, the limestone unlikely occurs in the high velocity (4.3 km/sec.) area since the velocity of the onshore fractured limestone is lower than the fresh limestone.

A part of the high velocity zone belongs to the positive magnetic anomaly zone. If limestone occurs in the high velocity area of more than 4.3 km/sec., it contradicts the fact that limestone is a non-magnetic substance.

(b) A positive gravity anomaly zone from Çatalagzi to Zonguldak corresponds to the limestone outcrops of the Cretaceous Aptian and the Barremian age. The same limestone is expected to occur in the positive gravity anomaly area offshore west of Zonguldak. Similarly, the limestone of the same age is expected to occur in the positive gravity anomaly area between the coast from Kozlu to Iliksu and 4 km offshore to the southwest. The distribution of the limestone is estimated by the above interpretation.

(2) Distribution of the Glauconitic Alternation

(a) The Gauconitic Alternation is expected to occur offshore in the positive magnetic anomaly area to the north of the limestone.

(b) The Glauconitic Alternation has lower magnetism than the tuff breccia. A glauconitif Alternation probably occurs to the south of the magnetic anomaly axis and its eastern margin probably extends and joins the onshore pillow lava.

(c) The seismic velocity analysis indicated that the Clauconitic Alternation has the highest velocity. Most of the high velocity zone of 4.3 km/sec. falls into the Glauconitic Alternation area or alternates with the glauconitic rock, therefore it is reasonable that the Glauconitic alternation occurs around the gravity anomaly axis.

(d) The Cretaceous Senomanian may occur in the area between the Glauconitic alternation and the limestone, but it's distribution is not certain due to a lack of data.

(3) Distribution of tuff breccia

(a) Tuff breccia probably occurs to the north of the pillow lava between the positive and negative gravity anomaly axis.

(b) Tuff breccia has the highest magnetism in the surveyed area and its distribution coincides with the magnetic anomaly axes on land.

(c) More than 4.0 km/sec. velocity is considered for the tuff breccia. Tuff breccia probably subcrops at the seafloor between 4.0 km/sec. velocity contour and positive magnetic anomaly axis. In the area between 4.0 km/sec. velocity contour and the negative magnetic anomaly axis, tuff breccia is probably deeply seared.

(d) Magnetic anomaly contours, and the positive and negative gravity anomaly axes suggest the occurrence of tuff breccia to the north.

suggest the occurrence of tuff breccia on the north.

(4) Distribution of andesite

(a) Rocks which cause magnetic anomaly in the area are tuff breccia, andesite, and intercalated glauconite. Andesite occurs onland between the positive and negative magnetic anomaly axes. Andesite may occur locally to the north of the tuff breccia, although few data support this.

(b) Undulated sea floor is observed on the seismic sections around the tuff breccia subcrop area. The further study will be required on this matter.

(5) Distribution of soft sediments

(a) Soft sediments probably occur to the north of 3.5 km/sec. velocity contour parallel and 2 – 4 km off the coast.

(b) A 3.5 km/sec. contour coincides with the 100 m water depth contour (transition of continental shelf and continental slope) and with truncation line of the green horizon (or 0.5 sec. contour of the grey green horizon). These facts are suggestive of the geological structure offshore.

(6) Nose structure to the north of Zonguldak

(a) Offshore north of Zongldak, the Green and Brown horizons make nose structures. The same structure is recognized on the magnetic survey results. Judging from the onshore geology and the conformable feature of these two reflections, the Green and the Brown horizon's are reflections at the top of the biotite angesite (Campanian Stage) and at the base of the Middle Cretaceous Agglomerate (Santonian – Coniacian Stage), respectively. The results of the velocity analysis showed that the two reflections the 700 – 1,000 m away each other. Their dips are similar to the Cretaceous formations observed onland.

1-3 Faults

(1) According to the Bouguer anomaly map

(a) Densely contoured part corresponds to the faulted area (for example, NE-SW contours in the SE part on Fig. 36).

(b) The same interpretation is employed around Zonguldak where steeply dipping structure parallel to the coast is faulted.

(c) A fault perpendicular to the coast and cut through the above structure around Kozlu certainly occurs. (Fig. 46).

(2) Isogam contours are winding offshore north of Iliksu, that is probably due to a fault.

(3) It was difficult to locate faults and to interprete structures on the reflection seismic sections.

(4) Low velocity sediment was found locally at the seafloor. A low velocity zone is generally interpreted as soft sediments or faulted zone. However, it is questionable to deliviate faults at this stage as the seismic grid is not dense enough.

1-4 Relationship of Coal Mine Location With Gravity Survey Result

(1) Negative gravity anomaly is observed where coal bearing formation lies shallow, as the result of that the specific gravity of the Carboniferous coal bearing formation is smaller than the limestone above and below it. Therefore it is reasonable that the coal mine entries are concentrated in the gravitational basin on the residual gravity maps. (Figs. 47 & 48).

(2) On the contrary, coal bearing formation occurs in the positive gravity anomaly zone (specific gravity 2.67), which is covered by high gravity formations.

1-5 Drilling in the Underground and Geological Structure

(1) A fractured zone encountered at the No. 2 drilling in the adit-22926 seems to run in the NNW-SSE direction taking into consideration the result at the No. 1 drilling in the adit-22926. This zone is considered as part of the incirharman Fault from its strike.

(2) About 50 m squense at the No. 2 drilling hole from the fault at 69.15m to the total depth at 120.6m is composed of the steeply dipping (60° – 70°) first sized conglomeratic Karadon Formation which is correlated to about 200 m in thickness, steeply dipping (70° ±) Karadon Formation encountered beyond the Simal Fault in the adit-22727.

From here to the northern part of the Simal Fault, the Kozlu Coal-bearing Formation is faulted down by the above fault. (200 m in the east, 600 m in the center, 700 m in the west). As a result, the minable Büyük seam at the top of the Kozlu Coal-bearing Formation lies at -550 – -700 m and the formation beyond the fault dip steeply to the north.

1-6 Estimation of the Coal Reserves

The geological structure beyond the Simal Fault in the Kozlu Mine is shown on the depth contours of the Büyük seam, which is minable and develops at the top of the Kozlu Formation.

A possibility of the existence of minable coal seam other than the Büyük seam in this area is not certain by looking at the available geological data. However, main minable coal seams in the presently working mines consist from the bottom of 3 coal seams Çay (2 – 3 level mining), Acilik (2 level mining) and Sulu. The other coal seams are also mined locally where developed. A development of the other coal seam is difficult to estimate without a direct survey because the formation between Sulu and Büyük seam ii as thick as about 380 m (Fig. 28). Consequently, the reserve estimation beyond the Simal Fault is made on the Büyük seam followed by precondition presented on pages 127 and 128 (Fig. 25).

In place coal reserves of the Büyük seam is calculated as shown on the following table (Table 30) as about 6.28 million tons. The coal reserves in the deeper part of the A-block, where is mined at present should be divided into the measured and indicated coal reserves according to the distance from the confirmed line but since there remains some discussions to employ Japanese JIS for the Turkish coal mines, only the in place coal reserves are presented in this report. (Table 30).

2. RECOMMENDATIONS

2-1 Coal Reserve Calculation and Underground Drilling Survey

(1) Based on the available geological data and the drilling result at the adit-22926, the Büyük seam which is expected to develop in the geological block to the north of the Simal Fault and at the top of the Kozlu Coal-bearing Formation was studied and it's in place coal reserves was estimated at 6.3 million tons although accuracy was very rough. It will be a future problem prove a coal reserves as a various precondition is taken into account for the estimation.

(2) If the fault encountered at the No. 2 drilling at the adit-22926 is assumed as the Incirharman Fault, the Simal Fault which runs to the west of the above fault should be shifted to the north, resulting the southern block to this fault becoming larger and consequently coal reserved becoming greater. A drilling survey by horizontal drilling at –425 m level at the adit-22929 will be required.

(3) As the coal seam in this area dips 50° –max. 80°, a special mining technique will be required. Moreover, as a large part lies under the sea, a very careful consideration for a safety countermeasure plan will be necessary.

2-2 Several Problems in Future Seismic Exploration

Further consideration in how to obtain a more detailed information which is the major purpose of the present project is thought to be important. To achieve this, further examination for several problems involved in the stage of both data acquisition and processing, taking the specific lithology of the area into consideration, will be necessary. Some of these problems have been already pointed out by the preliminary survey team. (Geophysical study section – the Interim Report of Pre-Feasibility study on the coal development Project at the offshore area of Zonguldak coal field in the Republic of Turkey, 1981).

Though the present interpretation, the final seismic sections which were acquired and processed by MTA was carefully analysed and followings were pointed out.

(1) Velocity determination and the use of long streamer cable on the final seismic sections processed JAPEX in 1981, several deep reflection responses could be recognized while on those processed by M.T.A., any indications of deep events could hardly be defected. This was thought to be caused by insufficient stacking effect which resulted from the use of inadequate stacking velocities. In other words, normal move out time appeared to be not properly corrected. By all means, we have to know reliable stacking velocities.

Unfortunately, however, it was extremely difficult to obtain reliable stacking velocities because velocity distribution at the sea-floor in the area is extremely high and consequently the move-out-time is very small.

Moreover, occurrence of primary reflection is limited which make the determination of precise interval velocities very difficult. One approach to solve this difficulty will be the use of long streamer cable.

From this point of view – JICA Pre-Feasibility study team has recommended the use of 1,200 m long cable.

However, through the present interpretation the author had an impression that the use of a longer cable, for instance 2,400 m long cable, will lead to the good result of velocity analysis.

(2) Improvement of the display unit

Representation of the processed seismic waveform was considered to be one of the important factor in the record quality.

The contrast of the final section displayed by Goul d-5000, a dot-print type electro-static printer that is presently used in M.T.A. was very poor due to insufficient density per inch. Laser-beam type display unit with transparent film will be necessary to obtain more clear variable area type representation.

(3) Modification of the air gun source

It has been believed that a smaller acoustic energy, within the range of the penetration to the target depth, will produce better quality record as far as resolution is concerned.

Data used for the present interpretation were acquired with 70 cubic inch in total air gun volume.

If shacking was more effectively achieved by proper NMO correction as mentioned above, some improvement in the record quality can be expected even with 70 cubic inch air gun.

However, author believed that detection of the reflection events from the Palaeozoic or more directly from the coal seam, regardless of the resolution of the record should be aimed first of all and then, as a next step, improvement of the resolution should be examined.

One of the solution to improve energy penetration without loosing the resolution is the

use of the high-pressure air gun.

Needless to say, the total energy of the outgoing acoustic pulse is determined by pressure and total volume of the air gun.

Consequently if air gun pressure can be increased for instance up to 4,500 p.s.i., air gun volume can be decreased as far as constant energy is concerned. Moreover, with the high-pressure air gun, built-up time of the primary pulse can be shortened which means that outgoing pulse contain more high frequency components resulting in greater 'resolution' than the conventional airgun system.

(4) Use of the long airgun array

In order to increase rate of energy which penetrates downward into the sediment, a long airgun array should also be considered.

(5) In the stage of data processing, the use of conventional deconvolution filters which is a part of the wavelet processing technique would be recommendable.

2-3 Refraction Survey and Analysis for Fault Delineation

As a result of the seismic velocity analysis of the seafloor by refraction survey, there seems to be obtained an assumption that a low velocity zone may correspond to a fault fractured zone. However, to connect each low velocity zone, it is necessary to shorten the distance of each survey line from 1,000 m at this survey to 500 m or even smaller so as to improve the accuracy further. And also it would be of course essential to obtain good record to read first arrivals easily. Furthermore, if possible, the achievement of 2-way travel time recording would be more desirous.

2-4 Technical Training for E.K.I.'s Drilling Supervisor

Technical transfer of underground horizontal drilling could have been mostly achieved during the period of drilling operation of the present project for over seven months.

However, it would be recommended that further technical training be provided to E.K.I.'s drilling supervisor in Japan on basic techniques of deep drilling (especially horizontal) and its lithological interpretation.

REFERENCES AND LITERATURE

1) Sleeman J. A. (1954) : New Harbour Construction at Zonguldak by The Royal Netherlands Harbourworks Company, Amsterdam, Holland, Madan, Turk Yuksek Maden Mühendisleri Cemiyeti Mecumuasi, Sayi 20,21, 1953/54.

2) Sarp. B. (1961) : Zonguldak Bituminous Coal field, CENTO.

3) M.T.A. (1975) : 1:50,000 Geological Map of Zonguldak Fig. No.30923

4) Inoue, E. (1970,71) : Geology and Coal Reserves of Turkey, 1, 2, Geological News, No.191,197 Geological Survey of Japan.

5) Brinkmann, R. (1976) : Geology of Turkey, Elsevier Scientific Publishing Company.

6) M.T.A. (1975) : Zonguldak-Azdavay Bölgesi, Tas Komürü Aramalari Gravite Etüdü, Bouguer Anomali Haritasi, 1:100,000, No.30013

7) TMMOB (1978) : Türkiye 1 Kömür Kongresi, 23–27 Ocak, 1978, Maden Müh Odasi, Zonguldak, S.B.

8) Tokay, M. (1961) : Geological Structure of The Amasura Coal Field, CENTO.

9) Patijn R.S.H. (1954) : The Geology of Zonguldak-Kozlu Area of The North Anatolian Coal Field, Turk Yüksek Maden Mühendisleri Cemiyeti Yayin Komitesi Tarafindon Çikariler, Maden, Sayi 20–21, 1953/54.

10) Ogzu, M. (1974) : Kandilli-Cavuşağzi Alaninin Genelleştirilmiş Stragigrafi Kasiti, 1:2,000.

11) Yahşiman, K. (1961) : Palynolosical Study of Paltozoin Coal in Turkey, CENTO.

12) E.K.I. (1982) : Palynolosical Analysis on the Coal Samples (M.S.)

13) Ralli, G. (1933) : La Bassin Aouiller d'Héraclée

14) Baykal, A. F. (1970) : Historik Jeolojj, Istanbul Publising

15) Bojo, T. et al. (1979) : Technical Cooperation Report on Exploration of Offshore Area of Zonguldak Coal Field, Turkey.
Japan International Cooperation Agency JR 79–24

16) Patijn R.S.H. (1954) : A Geolosica Research in the Carboniferous of Göbü, Maden, Sayi 20–21, 1953/54.

17) Inoue, M. et al. (1981) : The Interim Report of Pre-Feasibility Study on The Coal Development Project at The Offshore Area of Zonguldak Coal Field in The Republic of Turkey.
Japan International Cooperation Agency (Geophysical Study Section)

18) Ozkal, K. (1961) : Practice of Hydraulic Sandstowing in Arumtçuk Coal Field, CENTO.

19) Bayrl, R. (1961) : Carbonitization Characteristics of Some Turkish Coal, CENTO.

20) Hosono, M. et al. (1970) : Report on Geophysical Prospecting of Offshore Area of Kozlu Coal Mine, Zonguldak Coal Field, Nittetsu Mining Consultants Co., Ltd. (Unpublished)

21) Bojo, T. : Geological Profile of Zonguldak Coal Field.

22) Inoue, M. : Susceptibility Measurements of Rocks of Zonguldak Coal Field.

23) M.T.A. : Susceptibility Measurements of Rocks of Zonguldak Coal Field.

24) E.K.I. : Density Measurement of Rocks of Zonguldak Coal Field.

25) Seya, K. (1959) : A New Method of Analysis in Gravity Prospecting Running Average Method.
Geophysical Exploration (Butsuti-Tanko).

26) Kato, M. (1975) : Analysis of Gravity Field and Total Magnetic Field and the Subterranean Structure Corresponding to them.
Geophysical Exploration (Butsuri-Tanko).

27) Ogawa, K. & Tsu, H. (1976) : Magnetic Interpretation Using Interactive Computer Graphic. Report of Technology Research Center.
J.P.D.C. No.3

28) Koulomzine, Th. : New Method for the Direct Interpretation of Magnetic Anomalies Caused by Inclined Dike of Infinite Length.
Geophysics. Vol.35, No.5

29) Peter, Leo J. (1949) : The Direct Approach to Magnetic Interpretation and its Practical Application.
Geophysics. Vol.14